

Gadolinium Neutron Capture Therapy (GdNCT) Agents from Molecular to Nano: Current Status and Perspectives

Son Long Ho, Huan Yue, Tirusew Tegafaw, Mohammad Yaseen Ahmad, Shuwen Liu, Sung-Wook Nam, Yongmin Chang,* and Gang Ho Lee*



Cite This: *ACS Omega* 2022, 7, 2533–2553



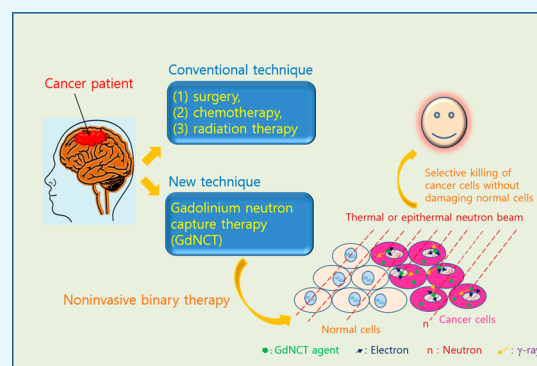
Read Online

ACCESS |

Metrics & More

Article Recommendations

ABSTRACT: ^{157}Gd (natural abundance = 15.7%) has the highest thermal neutron capture cross section (σ) of 254,000 barns (1 barn = 10^{-28} m²) among stable (nonradioactive) isotopes in the periodic table. Another stable isotope, ^{155}Gd (natural abundance = 14.8%), also has a high σ value of 60,700 barns. These σ values are higher than that of ^{10}B (3840 barns, natural abundance = 19.9%), which is currently used as a neutron-absorbing isotope for boron neutron capture therapy agents. Energetic particles such as electrons and γ -rays emitted from Gd-isotopes after neutron beam absorption kill cancer cells by damaging DNAs inside cancer-cell nuclei without damaging normal cells if Gd-chemicals are positioned in cancer cells. To date, various Gd-chemicals such as commercial Gd-chelates used as magnetic resonance imaging contrast agents, modified Gd-chelates, nanocomposites containing Gd-chelates, fullerenes containing Gd, and solid-state Gd-nanoparticles have been investigated as gadolinium neutron capture therapy (GdNCT) agents. All GdNCT agents had exhibited cancer-cell killing effects, and the degree of the effects depended on the GdNCT agents used. This confirms that GdNCT is a promising cancer therapeutic technique. However, the commercial Gd-chelates were observed to be inadequate in clinical use because of their low accumulation in cancer cells due to their extracellular and noncancer targeting properties and rapid excretion. The other GdNCT agents exhibited higher accumulation in cancer cells, compared to Gd-chelates; consequently, they demonstrated higher cancer-cell killing effects. However, they still displayed limitations such as poor specificity to cancer cells. Therefore, continuous efforts should be made to synthesize GdNCT agents suitable in clinical applications. Herein, the principle of GdNCT, current status of GdNCT agents, and general design strategy for GdNCT agents in clinical use are discussed and reviewed.



1. INTRODUCTION

Cancer has become one of the most dangerous diseases worldwide.¹ According to the National Cancer Institute, USA, there were more than 1.8 million new cancer occurrences and 600,000 deaths due to cancers in 2020 in the USA.¹ Effective cancer treatments have become an urgent demand in the field of medicine. Various cancer treatments such as surgery, chemotherapy, radiation therapy, immunotherapy, targeted therapy, and hormone therapy are now available. Cancer treatments depend on the cancer type and stage. For localized cancers at an early stage, surgery may be the standard choice for complete removal from the body, whereas for metastatic cancers at a late stage, a combination of the aforementioned treatments can be adapted to obtain the best results.

Neutron capture therapy (NCT) is considered promising among emerging cancer treatment techniques.² As a bimodal therapy, two essential components of NCT include NCT agents containing neutron-absorbing isotopes and a thermal (~ 0.025 eV) or epithermal (0.025–0.4 eV) neutron beam.

The neutron beam energy may decrease while passing through tissue,³ and neutrons are captured by the neutron-absorbing isotopes contained in preinjected NCT agents. The emitted energetic particles from neutron-absorbing isotopes destroy cancer cells by damaging DNAs (DNAs) inside cancer-cell nuclei through direct collision^{4a,b} or indirectly by generating reactive $\text{OH}\bullet$ radicals or OH^- ions via collision with water molecules inside cancer-cell nuclei, which reactively damage the DNAs.⁵ This binary therapy is noninvasive and kills cancer cells without damaging normal cells if NCT agents are selectively positioned only in cancer cells through targeting.

Received: November 22, 2021

Accepted: December 31, 2021

Published: January 12, 2022

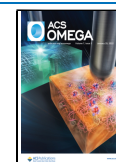


Table 1. GdNCT Agents Applied In Vitro

GdNCT agent	d^a (nm)	cell line	Gd-incubation concentration (washing option)	<i>in vitro</i> GdNCT result	ref
Gd-DO3A-butrol	–	Sk-Mel-28 cancer cell	0–30 mM Gd (no washing out of free Gd-DO3A-butrol from the cells)	Cancer-cell death increased with increasing Gd-incubation concentration.	11a
Gd-DTPA	–	TB10 GBM cancer cell	0–10 mg Gd/mL (washing out of free Gd-DTPA from the cells)	Cancer-cell death increased with increasing Gd-incubation concentration.	11b
Gd-DTPA	–	SW-1573 cancer cell	2.5 mM Gd (no washing out of free Gd-DTPA from the cells)	2.3 times higher cancer-cell death, compared to that obtained with no Gd-DTPA, and higher GdNCT effects than that obtained with γ -ray irradiation.	11c
Gd-DTPA	–	Chinese hamster V79 cell	51 ppm ^{157}Gd and ^{10}B (no washing out of free Gd-DTPA and BSH from the cells)	Higher Chinese hamster V79 cell death in Gd-DTPA solution, compared to that in BSH solution at the same ^{157}Gd and ^{10}B concentration.	11d
Gd-DTPA	–	C6 cancer cell	500 and 2500 ppm Gd (no washing out of free Gd-DTPA from the cells)	Cancer-cell death increased with increasing Gd-incubation concentration and neutron fluence.	11g
Gd-DTPA	–	C6 and CT26 cancer cells	0.5–50 ppm Gd (no washing out of free Gd-DTPA from the cells)	Cancer-cell death increased with increasing Gd and B on cancer-cell concentrations (additive effects of Gd and B on cancer-cell killings)	11h
Gd-DTPA/CaP nanocomposite (Gd-DTPA incorporated into calcium phosphate nanocomposite)	55	C-26 cancer cell	100 μM Gd (no washing out of free nanocomposites and free Gd-DTPA from the cells)	Incubation of C-26 cancer cells with extracellular Gd-DTPA/CaP nanocomposites and Gd-DTPA exhibited the similar 50% cancer-cell deaths.	14a
Gd-DTPA-liposome nanocomposite (Gd-DTPA encapsulated into various types of liposomes)	136–152	F98 and LN229 cancer cells	0.27–0.47 mg Gd/mL (no washing out of free nanocomposites from the cells)	Liposome composition-dependent Gd-concentrations in cancer cells and consequently, liposome composition-dependent cancer-cell deaths.	15c
Gd@C ₃₂ -PEG- <i>b</i> -PAMA nanoparticle [A Gd atom encapsulated inside metallofullerene (C ₃₂) and solubilized with PEG- <i>b</i> -PAMA]	20–30	C-26 cancer cell	63.4, 317, and 634 μM Gd (no washing out of free nanoparticles from the cells)	0%, 18%, and 24% C-26 cancer-cell deaths at incubation concentrations of 63.4, 317, and 634 μM Gd, respectively.	16
GdCo@CNP (Carbon-coated Gd-doped cobalt nanoparticle)	20–50 ^b	HeLa cancer cell	0.09677 μg nanoparticles (washing out of free nanoparticles from the cells)	55% HeLa cancer-cell death, which is higher than 52% cancer-cell death obtained with BC ₆₀ @CNPs.	17a
PEG-silica@Gd ₂ O ₃ nanoparticle [Gd oxide nanoparticle coated with polysiloxane and conjugated with PEG(COOH) ₂]	7.3 (Gd ₂ O ₃ core = 3.3 nm)	EL4-Luc cancer cell	0.0–0.3 mM Gd (washing out of free nanoparticles from the cells)	Cancer-cell death increased with increasing neutron beam irradiation dose (1.0–3.0 Gy) and Gd-incubation concentration (0.0–0.3 mM Gd).	17b
Gd ₂ O ₃ -PAA-Rho nanoparticle (Gd oxide nanoparticle coated PAA and conjugated with Rho)	14.3 (1.5 ^b)	U87MG cancer cell	0.5 mM Gd (washing out of free nanoparticles and Gd-DO3A-butrol from the cells)	28.1% higher cancer-cell death, compared to that of the (Gd-, n-) control cells, and 1.75 times higher cancer-cell death, compared to that obtained with Gd-DO3A-butrol.	17c

^aHydrodynamic diameter; ^bParticle diameter measured from TEM.

Table 2. GdNCT Agents Applied *In Vivo*

GdNCT agent	α^a (nm)	animal and cancer types (injection type) ^c	Gd-accumulation amount in cancer at irradiation time	<i>in vivo</i> GdNCT result	ref
Gd-DO3A-butrol	–	Mice, Sk-Mel-28 (i.t.)	1.2 mmol Gd/kg	Higher cancer-growth suppression, compared to that of the (Gd ⁻ , n ⁻) control group.	11a
Gd-DTPA	–	Mice, Jensen sarcoma (i.t.)	13,750 ppm Gd/g cancer	Complete cancer-volume regression for ~80% of mice tested.	11e
Gd-DTPA, Gd-BOPTA	–	Rats, 9L gliosarcoma (i.t.)	–	Gd-BOPTA exhibited a higher cancer-growth delay than Gd-DTPA, owing to a greater uptake of Gd-BOPTA in cancer than Gd-DTPA.	11f
Gd-DTPA	–	Rats, 9L gliosarcoma (i.v.)	–	A longer survival of the (Gd ⁺ , n ⁺) group (32 days) than the control (Gd ⁻ , n ⁻) group (16.4 days).	11g
Na ₂ (Gd-DTPA)	–	Dogs, oral melanoma and osteosarcoma (i.t.)	10–12 μ g ¹⁵⁷ Gd/mL	More effective, compared to BNCT for osteosarcoma, but less effective, compared to BNCT for melanoma.	11i
Gd-DO3A-BTA (Gd-DO3A conjugated with benzothiazole-aniline)	–	Mice, MDA-MB-231 (i.v.)	221 μ g/g cancer tissue	4.5 times smaller cancer volume, compared to that of the (Gd ⁻ , n ⁻) control group 60 days after irradiation.	11j
Gd-nanoCP nanocomposite (Gd-DTPA incorporated into chitosan nanocomposite)	430	Mice, B16F10 melanoma (i.t.)	2400 μ g Gd/mouse	A significant cancer-growth suppression, while Gd-DTPA mouse group showed a minor suppression.	12d
Gd-nanoCP-200 and Gd-nanoCP-400 nanocomposites [Gd-DTPA incorporated into chitosan nanocomposite made of different chitosan molecular weights (10 and 950 kDa)]	214 (Gd-nanoCP-200), 391 (Gd-nanoCP-400)	Mice, B16F10 melanoma (i.t.)	1500 μ g Gd/g cancer tissue (Gd-nanoCP-200) and 600 μ g Gd/g cancer tissue (Gd-nanoCP-400)	~two times smaller cancer volume of Gd-nanoCP-200, compared to that of Gd-nanoCP-400 on day 19 after irradiation.	12e
P272 and P454 nanocomposites [Gd-DOTA incorporated into poly(aspartic acid)-poly(ethylene glycol) nanocomposite (MW _{PEG} = ~12 and ~20 kDa)]	8.3 (P272), 9.8 (P454)	Mice, C-26 (i.v.)	1.8% of injected dose (P272), 3.2% of injected dose (P454)	P272 mouse group exhibited a higher GdNCT effect than P454 mouse group despite the higher Gd-accumulation of P454 nanocomposites in cancer, owing to a better penetration of smaller P272 nanocomposites inside cancer cells, compared to P454 nanocomposites.	13b
Ethylcellulose microcapsule containing Gd-DTPA	75–106 μ m	Mice, Ehrlich ascites (i.p.)	2.5 mg ¹⁵⁷ Gd/mL peritoneal fluid	Higher cancer-growth suppression and mice survival (~32% survival up to 60 days after irradiation), compared to the (Gd ⁻ , n ⁻) control mouse group (all control mice died prior to 13 days after irradiation).	13c
Gd-DTPA/CaP nanocomposite (Gd-DTPA incorporated into calcium phosphate nanocomposite)	55	Mice, C-26 (i.v.)	3.9% of injected dose	Five times smaller cancer volume, compared to that of the mouse group which received Gd-DTPA and thermal neutron.	14a
Gd-DTPA/CaP nanocomposite (Gd-DTPA incorporated into calcium phosphate nanocomposite)	60	Mice, C-26 (i.v.)	8.03 μ g Gd/g cancer (single injection) and ~17 μ g Gd/g cancer (three-time injection)	Three-time injection of Gd-DTPA/CaP led to higher uptake in cancer, but the cancer volume was similar to that of the single injection.	14b
Gd-HP-DO3A-Coatsome EL-01-N liposome nanocomposite (Gd-HP-DO3A encapsulated into Coatsome EL-01-N liposome nanocomposite)	100–300	Mice, C-26 (i.v.)	40.3 μ g/g cancer tissue	Four times smaller cancer volume, compared to that of the (Gd ⁻ , n ⁻) control mouse group 27 days after irradiation.	15b
PEGylated-liposome (Gd-DO3A-butrol encapsulated into PEGylated-liposome)	96.7	Mice, CT26 (i.v.)	–	43% cancer volume compared to that of the (Gd ⁻ , n ⁻) control mouse group 23 days after irradiation. Additional injections and irradiation 10 days after the first irradiation led to higher cancer-growth suppressions.	15d
Gd ₂ O ₃ -PAA-RGD (Gd oxide nanoparticle coated with PAA and conjugated with RGD)	12.1 (1.8 ^b)	Mice, U87MG (i.v.)	2.2 μ g/g cancer tissue	8 times smaller cancer volume, compared to that of the (Gd ⁻ , n ⁻) control mouse group on day 25 after irradiation.	17d

^aHydrodynamic diameter; ^bparticle diameter measured from TEM. ^cInjection type: i.v. = intravenous injection, i.t. = intratumoral injection, and i.p. = intraperitoneal injection.

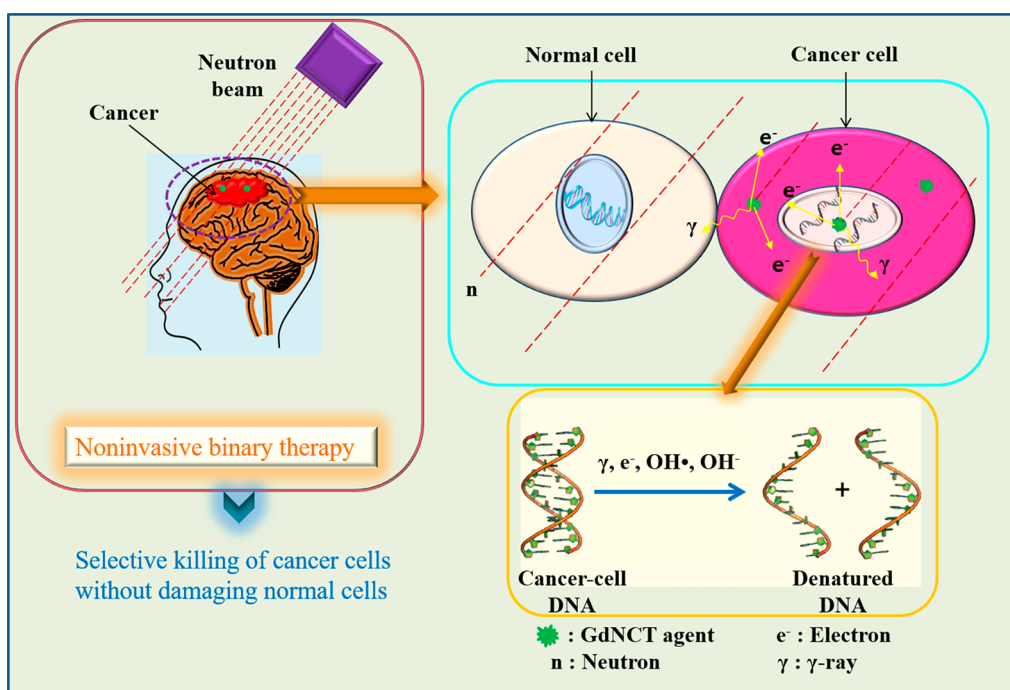


Figure 1. Energetic particles (electrons and γ -rays) kill cancer cells by damaging DNAs inside cancer-cell nuclei by direct collision or indirectly by generating reactive $\text{OH}\bullet$ radicals or OH^- ions through collision with water molecules inside the nuclei, which reactively damage the DNAs.

The first NCT was based on a stable (nonradioactive) isotope, ^{10}B (natural abundance = 19.9%), which was proposed by Gordon Locher in 1936,^{6a} and this BNCT has since been widely investigated.^{6b} The ^{10}B possesses a thermal neutron capture cross section (σ) of 3840 barns (1 barn = 10^{-28} m²). After the absorption of neutrons, the excited ^{11}B emits a high linear energy transfer α -particle (^4He) and leaves a lithium-7 nuclei (^7Li), which is termed $^{10}\text{B}(n, \alpha)^7\text{Li}$.⁷ Both α and ^7Li particles have penetration depths in the range of 4–9 μm in tissue,⁷ corresponding to cell dimensions. Thus, they can damage cancer-cell DNAs through direct collision, if they are generated inside cancer-cell nuclei. Presently, two clinically approved BNCT agents are available. They include sulfhydryl borane (BSH; $\text{Na}_2\text{B}_{12}\text{H}_{11}\text{SH}$) and *p*-dihydroxyboryl-phenyl-alanine (BPA; $\text{C}_9\text{H}_{12}\text{BNO}_4$).⁷

However, the rising interest in the application of Gd as gadolinium neutron capture therapy (GdNCT) agents originates from an extremely large σ value of 254,000 barns for ^{157}Gd (natural abundance = 15.7%), which is the highest value among stable isotopes in the periodic table.⁸ Another stable isotope, ^{155}Gd (natural abundance = 14.8%), possesses a σ value of 60700 barns, which is higher than that of ^{10}B .⁸ Both isotopes can contribute to NCT if natural Gd is used in GdNCT agents. In addition, GdNCT agents can serve as magnetic resonance imaging (MRI) contrast agents because of the high longitudinal proton spin relaxivities of Gd,⁹ implying that GdNCT agents can be used as theranostic (MRI-guided GdNCT) cancer agents.^{10a} This is another advantage of Gd over B. For B, MRI-guided BNCT can be conducted by bonding Gd-chemicals to BNCT agents,^{10b} with the dose enhancement.^{10c}

To take advantage of the considerably large σ values of ^{157}Gd and ^{155}Gd , significant efforts have been focused on applying various Gd-chemicals in GdNCT.^{11–17} Commercial molecular MRI contrast agents (Gd-chelates) have been naturally applied in GdNCT.^{11a–i} Thereafter, various Gd-

chemicals such as modified Gd-chelates,^{11j} nanocomposites containing Gd-chelates,^{12–15} fullerenes containing Gd,¹⁶ and solid-state Gd-nanoparticles¹⁷ were synthesized and applied in GdNCT, because commercial Gd-chelates exhibited poor accumulation in cancer cells, making them unsuitable for clinical application.^{5,10a,11b,14b} All GdNCT agents applied to *in vitro* (Table 1) and *in vivo* experiments (Table 2) exhibited GdNCT effects, and the degree of the effects depended on the GdNCT agents used. Several performance comparison studies with BNCT have been also conducted.^{11d,i,17a} Therefore, it is valuable to overview GdNCT agents investigated to date and address their current status. This review may help researchers to define future research directions in GdNCT agents. In addition, the principle of GdNCT and general design strategy for GdNCT agents suitable in clinical application are discussed.

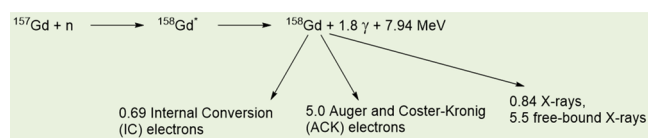
2. PRINCIPAL ELEMENTS OF GDNCT

2.1. Principle of GdNCT as a Bimodal Therapy.

GdNCT is a bimodal therapy,² as shown in Figure 1. First, a GdNCT agent is injected into a cancer patient. When the injected GdNCT agent has reached highest accumulation in the cancer cells, a thermal (~ 0.025 eV) or epithermal (0.025–0.4 eV) neutron beam² is irradiated to the cancer cells to kill them.

2.2. Neutron Absorbing Isotopes. Naturally occurring Gd comprises six stable isotopes (natural abundances = 99.8%) and one minor radioactive isotope (natural abundance = 0.2%, half-life = 1.08×10^{14} y).^{18a} Therefore, Gd is safe and can be used in GdNCT agents. Among them, ^{157}Gd and ^{155}Gd possess very high σ values applicable in GdNCT.⁸

Equation 1 shows the neutron capture reaction of ^{157}Gd . As shown in eq 1, when irradiated with a neutron beam, the ^{157}Gd undergoes a $^{157}\text{Gd}(n, \gamma)^{158}\text{Gd}$ NC reaction to yield the excited $^{158}\text{Gd}^*$, which decays into ^{158}Gd and emits γ -rays (energy ≈ 1.4 MeV, penetration depth = a few centimeters).^{18b} During



this process, the γ -rays may remove core-shell electrons of ^{158}Gd , and the removed electrons are called internal conversion (IC) electrons (70.1 keV, ~ 0.1 nm). Thereafter, Auger and Coster-Kronig (ACK) electrons (0.8 keV, ~ 20 nm) and certain X-rays are generated after the IC electrons are emitted.^{18b} In addition, ^{155}Gd undergoes a similar NC reaction to ^{157}Gd .^{18c} The generated energetic particles such as ACK and IC electrons and γ -rays kill cancer cells by damaging DNAs inside cancer-cell nuclei,⁴ as shown in Figure 1. Considering that γ -rays can damage both cancer and normal cells, owing to their long penetration depth and high energy, the ACK and IC electrons (particularly ACK electrons) are a preferred choice for the killing of cancer cells. Therefore, GdNCT agents should be accumulated inside cancer cells, preferably inside cancer-cell nuclei. Reactive $\text{OH}\bullet$ radicals or OH^- ions produced by collisions between the aforementioned energetic particles and water molecules inside cancer-cell nuclei can also kill cancer cells through their reaction with DNAs,⁵ as shown in Figure 1.

2.3. Gd-Dose. It was suggested that an appropriate ^{157}Gd -concentration in cancer should be in the range of 50–200 μg $^{157}\text{Gd}/\text{g}$ cancer tissue (or 50–200 ppm ^{157}Gd),^{15a} but less than 1000 ppm ^{157}Gd because ^{157}Gd accumulated in superficial cancer cells can quickly deplete neutrons, causing deeply seated cancer cells to be insufficiently irradiated with neutrons.^{14b,15a} For instance, a higher Gd-accumulation in cancer was achieved via multiple intravenous injections of GdNCT agents into mice, compared to that obtained with a single injection. However, similar cancer-growth suppressions were observed for both cases.^{14b} Additionally, a low GdNCT effect was observed as a result of the shielding effect of thermal neutrons by a high ^{157}Gd -concentration in dogs with oral melanoma cancer.¹¹ⁱ

The intravenous Gd-injection dose of GdNCT agents is similar to that used in the clinical MRI of commercial Gd-chelates, which is 0.1–0.3 mmol Gd/kg.^{10a} Considering the

natural abundance of ^{157}Gd (15.7%) and assuming 100% accumulation of the injected Gd (injection dose = 0.1 mmol Gd/kg) in 1.0 mg of cancer, 98.6 ppm of ^{157}Gd will be accumulated in cancer cells with a single injection, which is within the required ^{157}Gd -concentration for GdNCT.^{15a}

However, because the accumulation percentage of the injected Gd in cancer is generally lower than 100%, multiple injections of GdNCT agents might be needed to achieve the required ^{157}Gd -concentration in cancer. Another way to improve the ^{157}Gd -accumulation is to use ^{157}Gd -enriched GdNCT agents. In addition, the conjugation of cancer-targeting ligands to GdNCT agents can improve ^{157}Gd -accumulation. Gd-nanoparticles will be another choice for this improvement because they can deliver a large amount of Gd per nanoparticle to cancer.

2.4. Thermal and Epithermal Neutron Beam Source and Dose. Previously for NCT, a nuclear reactor was the most common neutron beam source.^{19a} However, the accelerator (cyclotron or linear)^{19b} has become more common than the nuclear reactor because the accelerators can be easily installed in hospitals or institutes because of their small size, low cost, easy installation, high safety, and simple operation, compared to the nuclear reactor. The GdNCT experiment is performed in a beam room isolated from the neutron beam source by a thick heavy concrete or lead plate to block unwanted neutrons.^{19a} To understand the GdNCT process, a schematic illustration of GdNCT using a linear accelerator is shown in Figure 2.^{19c} As shown, a high-energy proton beam hits the beryllium or lithium target to generate neutrons, which slow down to thermal or epithermal neutrons by a moderator and are narrowed down by a collimator to align toward the cancer cell.

The σ value of elements drops as neutron kinetic energy increases.³ Thus, neutrons with lower kinetic energies are preferred for GdNCT. However, the neutron beam energy drops while passing through the body, and cold neutrons (0–0.025 eV) are not suitable for GdNCT because most of them stop at or around the skin. Neutrons with higher energies than cold neutrons should be used: thermal neutrons (~ 0.025 eV) can be used for shallow cancers, while epithermal neutrons (0.025–0.4 eV) can be used for deeply positioned cancers in the body.^{19d}

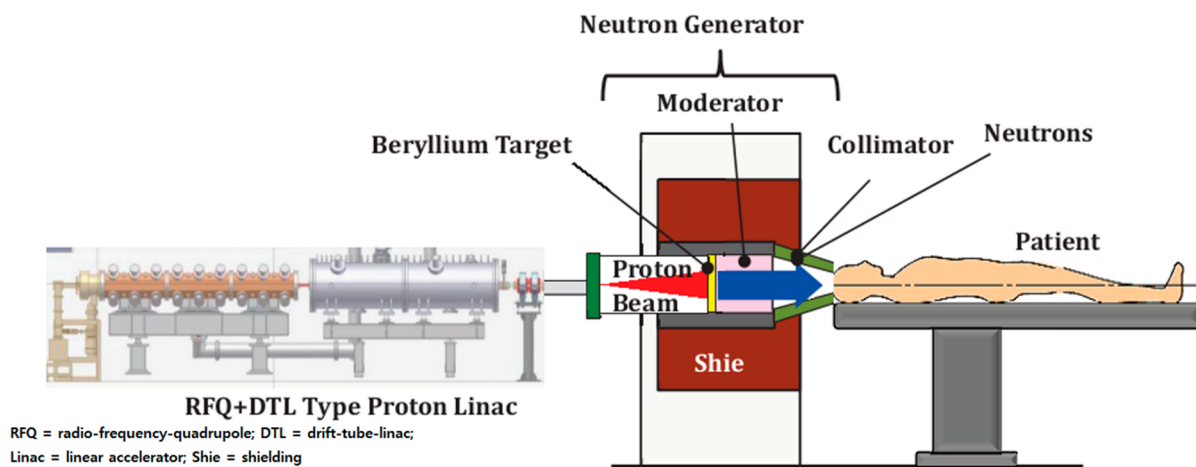


Figure 2. Schematic diagram of GdNCT operation using a linear accelerator as a thermal and epithermal neutron beam source. Adapted with permission from ref 19c. Copyright 2013 Pioneer Bioscience Publishing Company.

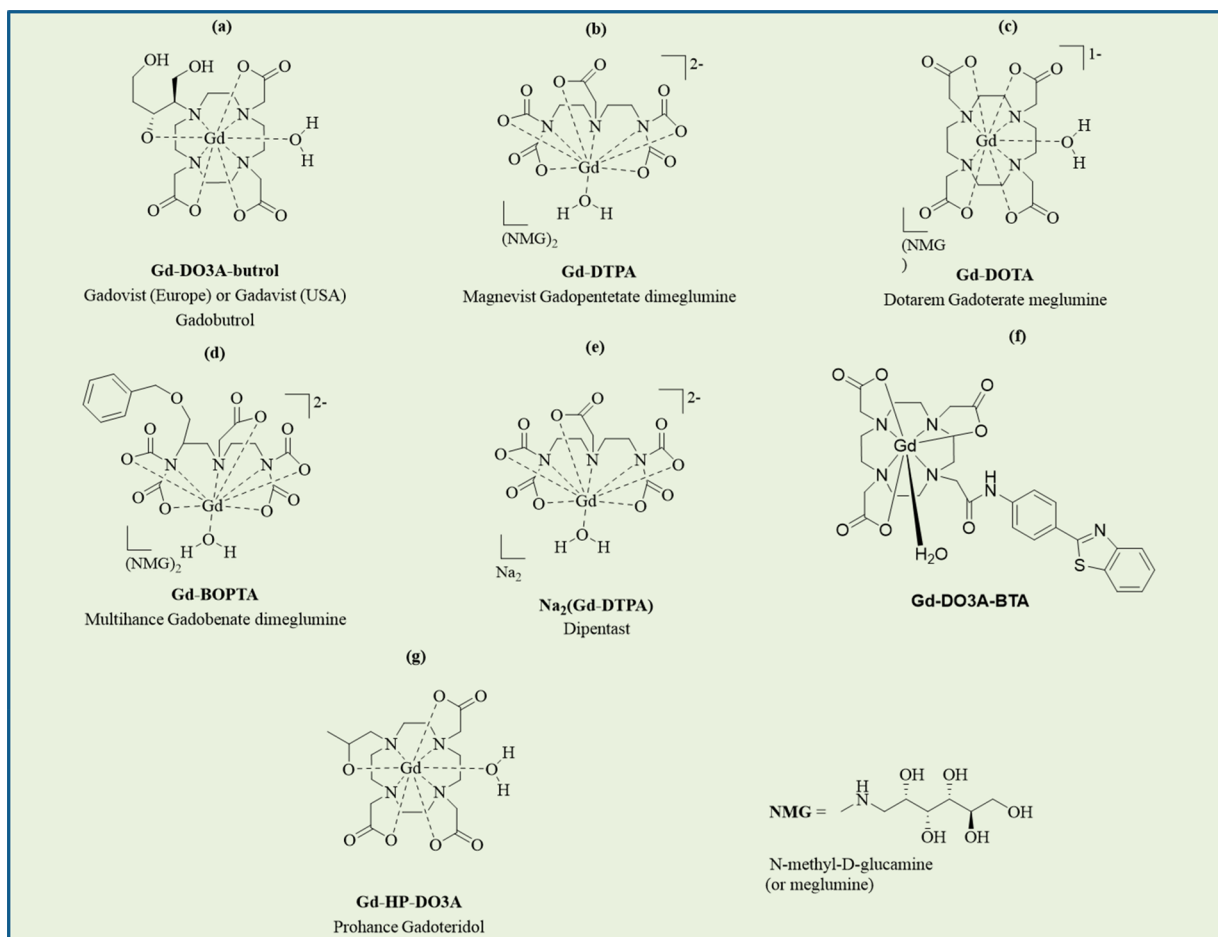


Figure 3. (a) Gadovist. (b) Magnevist. (c) Dotarem. (d) Multihance. (e) Dipentast. (f) Gd-DO3A-BTA (modified Gd-chelate). (g) Prohance. Gd-chelates in (a), (b), (c), (d), and (g) are clinically approved.

The σ values of common body elements such as ^1H (0.333 barns), ^{12}C (0.0035 barns), ^{14}N (1.83 barns), ^{16}O (0.00019 barns), ^{56}Fe (2.57 barns), and ^{20}Ca (0.4 barns) are generally minimal, compared to those of ^{157}Gd and ^{155}Gd .² The neutron beam absorption by these elements is negligible; therefore, the neutron beam will not be harmful to the body unless a high dose is used. Bridot et al. confirmed this from *in vitro* cellular GdNCT experiments, where a thermal neutron beam dose up to 3.0 Gy was not toxic to cancer cells, although it was toxic at 7.0 Gy.^{17b} The dose unit was either fluence (flux \times time, neutrons cm^{-2}) or gray (Gy, absorbed J per matter kg). The clinical data of a thermal or epithermal neutron beam dose for GdNCT has not been reported because there have been no clinical GdNCT trials to date. However, that used for mice experiments was on the order of 10^{12} neutrons cm^{-2} .^{13b,14a} In comparison, the clinical data of a neutron beam dose used for BNCT was in the range of 10^9 – 10^{12} neutrons cm^{-2} (~ 10 Gy),^{19e} and that used for mice BNCT experiments was 10^{12} – 10^{13} neutrons cm^{-2} .^{19f} Therefore, the clinical data of the dose for GdNCT would be similar to that used for BNCT.

3. OVERVIEW OF PREVIOUSLY USED GDNCT AGENTS

3.1. General Points. The GdNCT agents investigated to date range from molecular to nano.^{5,11–17} They were applied to GdNCT *in vitro* (Table 1) and *in vivo* (Table 2). Considering the poor accumulation of commercial Gd-chelates in cancer cells,^{5,10a,11b,14b} modified Gd-chelates^{11j} and nano-

materials^{12–17} have been synthesized to overcome these limitations. They exhibited higher Gd-accumulations in cancer cells *in vitro* and *in vivo*, compared to those of commercial Gd-chelates. Consequently, they have higher cancer-cell deaths than commercial Gd-chelates.

3.2. Gd-Chelates. **3.2.1. Clinically Approved Gd-Chelates: Gd-DO3A-butrol, Gd-DTPA, Gd-DOTA, and Gd-BOPTA.** Four clinically approved Gd-chelates such as Gd-10-(1,3,4-trihydroxybutan-2-yl)-1,4,7,10-tetraazacyclododecane-1,4,7-tricarboxylate (Gd-DO3A-butrol) (Gadovist, Bayer Healthcare Pharmaceuticals Inc., Germany) (Figure 3a); Gd-diethylenetriaminepentaacetic acid (Gd-DTPA) (Magnevist, Bayer Healthcare Pharmaceuticals Inc., Germany) (Figure 3b); Gd-tetraazacyclododecanetetraacetic acid (Gd-DOTA) (Dotarem, Guerbet, France) (Figure 3c), and Gd-benzyloxypropionictetraacetate (Figure 3d) (Multihance, Bracco, USA) have been applied in GdNCT in intact form *in vitro*^{11a–d,g,h} or *in vivo*.^{11a,e–g}

Hoffmann et al. applied Gd-DO3A-butrol to GdNCT *in vitro* and *in vivo*.^{11a} For *in vitro* applications, a thermal neutron beam was irradiated onto human melanoma cancer cells (Sk-Mel-28) suspended in a Gd-DO3A-butrol solution (0, 10, and 30 mM Gd). A delay in the proliferation of the Sk-Mel-28 cancer cells was observed after the irradiation and increased with an increase in the Gd-concentration, demonstrating GdNCT effects, whereas cells with no irradiation exhibited the same cancer-cell growth, regardless of their Gd-concentrations

in solution (Figure 4a). For *in vivo* GdNCT experiments, Gd-DO3A-butrol was intratumorally injected into Sk-Mel-28 cancer-bearing mice inoculated at one of the hind limbs to maximize the uptake of Gd-DO3A-butrol by cancer cells with a high injection dose of 1.2 mmol Gd/kg. A significant delay in the cancer volume growth was observed after irradiation,

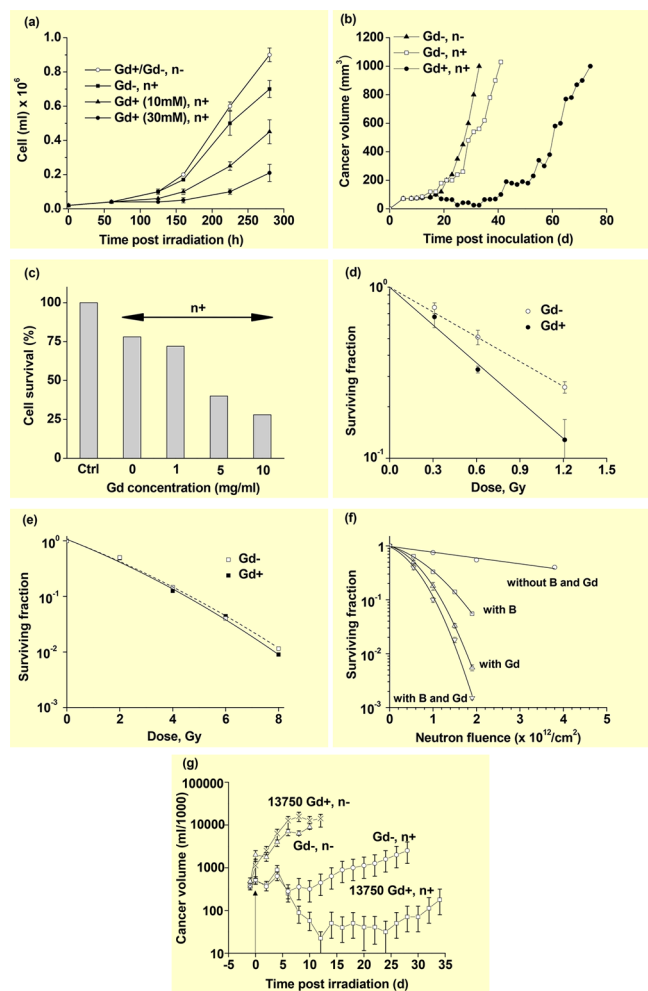


Figure 4. (a) *In vitro* Sk-Mel-28 cancer-cell growth curves (cells/mL) in Gd-DO3A-butrol solutions as a function of hours after thermal neutron beam irradiation ($n = 3$). (b) *In vivo* mice cancer volume (mm^3) growth curves as a function of days after thermal neutron beam irradiation ($N = 5-6$). Reproduced with permission from ref 11a. Copyright 1999 Lippincott Williams & Wilkins, Inc. (c) *In vitro* TB10 GBM cancer-cell survival histogram (%) as a function of the Gd-incubation concentration (mg Gd/mL) after free Gd-DTPA was washed out from the cells prior to irradiation [normalized using (Gd-, n-) control cells] ($n = 4$). Reproduced with permission from ref 11b. Copyright 2001 American Association for Cancer Research. (d) *In vitro* SW-1573 cancer-cell survival curves with and without 2.5 mM Gd-DTPA in media as a function of the thermal neutron beam irradiation dose. (e) *In vitro* SW-1573 cancer-cell survival curves with and without 2.5 mM Gd-DTPA in media as a function of the γ -ray irradiation dose. Reproduced with permission from ref 11c. Copyright 2006 Spandidos Publications. (f) *In vitro* Chinese hamster V79 cell-surviving fractions with and without Gd-DTPA and BSH in media as a function of the thermal neutron beam dose. Reproduced with permission from ref 11d. Copyright 2000 Urban and Vogel. (g) *In vivo* cancer volume (logarithmic scale) in milliliters of four mouse groups as a function of days after irradiation. Reproduced with permission from ref 11e. Copyright 1995 Elsevier.

compared to that in the control group with no Gd-DO3A-butrol and irradiation, demonstrating GdNCT effects (Figure 4b). For *in vitro* and *in vivo* experiments, the irradiation with no Gd-DO3A-butrol slightly suppressed the cancer growth, indicating slight toxicity in the irradiation to cancer cells because of tiny absorptions of thermal neutrons by cell elements (H, C, O, N, etc.) at the irradiation dose used. This was commonly observed in GdNCT experiments.^{11b,c,g,17b,d} However, the irradiation was not toxic at a low dose.^{17b}

De Stasio et al. incubated TB10 human glioblastoma multiforme (GBM) cells with Gd-DTPA and Gd-DOTA and observed that 84% and 56% of the TB10 GBM cell nuclei contained Gd-DTPA and Gd-DOTA, respectively, 72 h after cell cultures.⁵ In rats with intracerebrally implanted C6 glioma brain cancer, 47% and 85% of cell nuclei had Gd-DOTA 1.0 h after single and double tail vein injection of Gd-DOTA, respectively (single-injection dose = 0.4 mmol Gd/kg). For patients with GBM brain cancer, Gd-DTPA was intravenously injected into patients (injection dose = 0.1 mmol Gd/kg) 1–2 h prior to cancer excision. Only 6.1% of the cancer-cell nuclei contained Gd-DTPA, suggesting a considerably low efficacy of Gd-DTPA and Gd-DOTA as GdNCT agents for humans because of their poor accumulation performance in cancer. This is because both Gd-chelates are extracellular and lack cancer-cell targeting abilities.^{20a} In addition, they are rapidly excreted through the renal system within a few hours after injection.^{20b} De Stasio et al. also reported the incubation of TB10 GBM cells with Gd-DTPA (0–10 mg Gd/ml) for 72 h.^{11b} After washing out the free Gd-DTPA from the cells, thermal neutron beam irradiation was performed. Cancer-cell deaths increased with an increase in the incubation Gd-concentration (Figure 4c), confirming GdNCT effects. As shown, ~20% cell death of the irradiated cells with no Gd-DTPA was observed, owing to a slight absorption of thermal neutrons by cell elements, as observed in other studies.^{11a,c,g,17b,d}

Franken et al. reported that human squamous lung carcinoma cancer cells (SW-1573) suspended in Gd-DTPA media of 2.5 mM Gd exhibited a 2.3-fold higher cancer-cell death, compared to those of the control cells with no Gd-DTPA after irradiation (Figure 4d).^{11c} The cancer-cell death with no Gd increased with an increasing irradiation dose because of a slight absorption of thermal neutrons by cell elements,^{11a,b,g,17b,d} implying that a high irradiation dose should be avoided in GdNCT. However, the irradiation was not toxic at a low dose.^{17b} Notably, these cancer-cell deaths were higher than those obtained using γ -ray irradiation (Figure 4e), suggesting that among energetic particles produced from GdNCT, ACK and IC electrons are more effective than γ -rays in cancer-cell killing. This further suggests that a considerably effective GdNCT result can be obtained if GdNCT agents are accumulated inside cancer cells, preferably inside cancer-cell nuclei because of short penetration depths of the ACK and IC electrons.⁷

Tokuuye et al. observed higher Chinese hamster V79 cell deaths when the cells were suspended in Gd-DTPA solution, compared to that when suspended in BSH solution at the same ¹⁵⁷Gd and ¹⁰B concentrations after irradiation (Figure 4f).^{11d} This suggests that GdNCT might be more effective than BNCT.

Khokhlov et al. conducted *in vivo* GdNCT experiments on Jensen sarcoma-bearing mice inoculated in their right thighs.^{11e} The cancer volume reached 10–15 mm in diameter

7–8 days after a subcutaneous injection of 5×10^6 cancer cells prepared in 0.5 mL of M0393 medium. They intratumorally injected Gd-DTPA to reach 13,750 ppm Gd in the cancer cells prior to the thermal neutron beam irradiation and observed regression in cancer volume after irradiation (Figure 4g). As shown, a complete regression in the cancer volume was observed for approximately 80% of the (Gd+, n+) mouse group 7 days after irradiation. The (Gd-, n+) mouse group showed a temporal cancer volume regression; however, it subsequently increased. Both the (Gd-, n-) and (Gd+, n-) mouse groups showed a natural cancer-volume growth. Considering the extracellular properties of Gd-DTPA,^{20a} the observed GdNCT effects were mostly due to γ -rays and high-energy IC electrons, not low-energy IC and ACK electrons. These results suggested that Gd-DTPA might be an effective GdNCT agent for surface-seated cancers with intratumoral injection at a high Gd-dose prior to irradiation.

Matsumura et al. compared *in vivo* GdNCT efficacy between Gd-DTPA and Gd-BOPTA using 9L gliosarcoma-bearing rats inoculated in hind legs.^{11f} Both Gd-DTPA and Gd-BOPTA were intratumorally injected into the cancer to maximize Gd uptake (injection dose = 0.05 mmol Gd/g cancer). They observed a higher cancer-growth delay in Gd-BOPTA group, compared to that of the Gd-DTPA group, owing to a greater uptake of Gd-BOPTA in cancer than Gd-DTPA; this is because of the benzene ring in Gd-BOPTA (Figure 3d) which allowed more cellular uptake in cancer cells,^{20c} compared to extracellular Gd-DTPA.^{20a}

Takagaki et al. observed significant *in vitro* and *in vivo* GdNCT effects using Gd-DTPA.^{11g} For C6 cancer cells suspended in Gd-DTPA solutions, the cancer-cell surviving fraction decreased with an increase in Gd concentration (0, 500, and 2500 ppm) and in thermal neutron fluence in the range of $(0-6.5) \times 10^{12}$ neutrons/cm². For *in vivo* experiments on 9L brain cancer-bearing rats, the thermal neutron beam was irradiated for 45 min after intravenous injection (1.0 mmol Gd/mouse). Gd-DTPA (0.5 mmol Gd/mouse) was additionally injected 22.5 min after irradiation to boost Gd-concentration in brain cancer. They observed a considerably prolonged survival of 32 days after irradiation, compared to 16.4 days for the control (Gd-, n-) group.

Yoshida et al. investigated additive NCT effects on C6 and murine colorectal carcinoma (CT26) cancer cells suspended in BPA (0–40 ppm B) and Gd-DTPA (0–50 ppm Gd) mixture solutions.^{11h} They observed additive NCT effects by BPA and Gd-DTPA. A similar additive NCT effect was observed in Chinese hamster V79 cells suspended in Gd-DTPA and BSH solutions.^{11d} These results are attributed to the enhanced absorption of thermal neutrons to kill cells by ¹⁵⁷Gd, ¹⁵⁵Gd, and ¹⁰B.^{10c}

3.2.2. Nonclinically Approved Na₂(Gd-DTPA). Mitin et al. applied Na₂(Gd-DTPA) (Dipentast, Figure 3e) to *in vivo* GdNCT experiments on dogs with malignant oral melanoma and osteosarcoma cancers.¹¹ⁱ They intratumorally injected it to obtain an accumulation concentration of 10–12 $\mu\text{g } ^{157}\text{Gd/mL}$ in the cancer cells prior to the thermal neutron beam irradiation. In comparison, they intravenously and intra-arterially injected BPA in the melanoma and osteosarcoma cases, respectively, to obtain 28.5 ppm ¹⁰B in the cancer cells ~2 h prior to irradiation. The results indicated that BNCT was more effective for the oral melanoma, while GdNCT was more effective for the osteosarcoma. They elucidated that γ -rays could effectively kill interstitial cancers, such as osteosarcoma,

because Dipentast is intercellular, whereas the α -particles could effectively kill soft and superficial cancers, such as oral melanoma, because BPA is intracellular. In addition, they observed that at higher Gd-accumulation concentrations exceeding 12 $\mu\text{g } ^{157}\text{Gd/mL}$, a low GdNCT effect was observed as a result of the shielding effect of thermal neutrons by extra ¹⁵⁷Gd. This was consistent with the observation that a three-time injection of Gd-DTPA nanocomposites caused a higher uptake in the cancer cells; however, the GdNCT effect was similar to the single-injection case.^{14b}

3.2.3. Modified Gd-Chelates: Gd(DO3A)-BTA. To overcome the low accumulation of commercial Gd-chelates in cancer cells because of their extracellular and inadequate cancer-targeting properties,^{20a} Jung et al. synthesized Gd-1,4,7,10-tetraazacyclo-dodecane-1,4,7-trisacetic acid (DO3A)-benzothiazole-aniline (BTA) (Figure 3f) and applied it to the *in vivo* GdNCT for mice inoculated with human breast cancer (MDA-MB-231) cells.^{11j} Gd(DO3A)-BTA was cancer-specific and intracellular because of the BTA moiety and consequently showed brighter T₁ MR images and higher contrast-to-noise ratios (CNRs) in the cancer cells, compared to those obtained with Gd-DOTA in mice experiments (Figure 5a).^{21a} For *in vivo* GdNCT experiments, Gd(DO3A)-BTA was intravenously injected into MDA-MB-231 cancer-bearing mice tails (injection dose = 0.1 mmol Gd/kg).^{11j} This injection dose caused a maximum uptake of 221 $\mu\text{g Gd/g}$ cancer tissue 6 h after injection, corresponding to 34.7 $\mu\text{g } ^{157}\text{Gd/g}$. This Gd-accumulation was close to the optimal ¹⁵⁷Gd-concentration of 50–200 $\mu\text{g } ^{157}\text{Gd/g}$ cancer tissue for GdNCT.^{15a} Sixty days after the irradiation, the cancer volume of the (Gd+, n+) mouse group was the least among the four mouse groups, as shown in the T₁ MR images and photographs (Figure 5b). In addition, it was 4.5 times smaller than the cancer volume of the (Gd-, n-) control mouse group (Figure 5c), thereby confirming GdNCT effects.

3.3. Nanocomposites or Nanocarriers Containing Clinically Approved Gd-Chelates. To increase Gd-accumulation and Gd-retention in cancer, nanocomposites or nanocarriers containing large amounts of commercial Gd-chelates have been prepared as GdNCT agents.^{12–15} These include polymeric nanocomposites, such as chitosans,^{12a–e} dendrimers,^{13a} poly(amino acids),^{13b} and cellulose microcapsules;^{13c} mineral nanocomposites, such as calcium phosphates;^{14a,b} and lipid-based nanocomposites, such as liposomes.^{15a–d}

3.3.1. Chitosan Nanocomposites. Chitosan is a cationic polysaccharide derived from the deacetylation of chitin and has been widely applied in biomedical and pharmaceutical areas because of its natural abundance, biocompatibility, biodegradability, nontoxicity, and enhanced permeability.^{21b} Using an emulsion-droplet coalescence technique, Gd-DTPA-loaded chitosan nanoparticles (Gd-nanoCPs) were prepared through electrostatic bonding between the carboxylic groups of Gd-DTPA and amine groups of chitosan.¹² Shikata et al. observed a considerably higher accumulation of Gd-nanoCPs [hydrodynamic diameter (*a*) = 426 nm] in mouse fibroblast (L929), malignant melanoma (B16F10), and squamous carcinoma (SCC-VII) cells, compared to those obtained with Gd-DTPA after washing out free nanoparticles and Gd-DTPA from the cells with a phosphate buffer saline (PBS) solution 12 h after cellular incubation (Figure 6a).^{12a} In a similar experiment using Gd-nanoCPs (*a* = 425 nm), Fujimoto et al. observed an approximately three times higher Gd-concentration of 30.5 μg

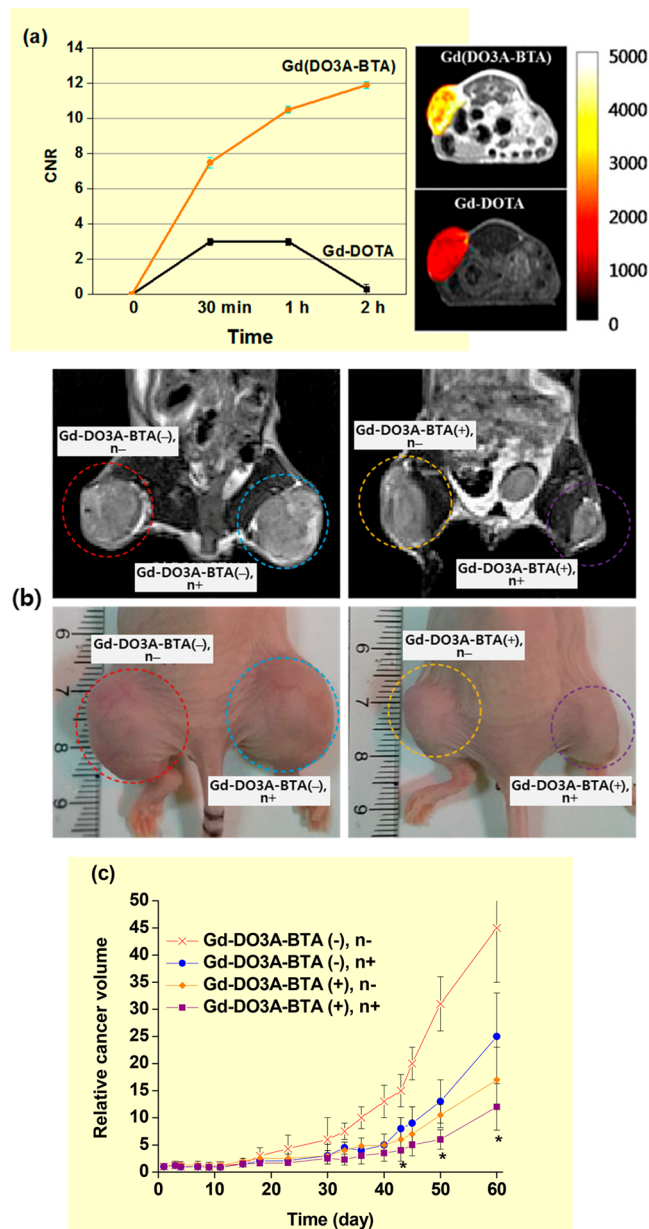


Figure 5. (a) Plots of contrast-to-noise ratios (CNRs) of MDA-MB-231 cancers in mice with time after intravenous injection with Gd(DO3A)-BTA and Gd-DOTA (left) and T₁ MR images of cancers in mice 1.0 h after intravenous injection (right). Adapted and reproduced from ref 21a. Copyright 2013 American Chemical Society. (b) T₁ MR images (top) and photographs (bottom) of cancers on mouse thighs 60 days after thermal neutron beam irradiation: from the left, [Gd-DO3A-BTA(-), n-], [Gd-DO3A-BTA(-), n+], [Gd-DO3A-BTA(+), n-], and [Gd-DO3A-BTA(+), n+]. (c) Plots of relative cancer volumes ($V_{\text{day}}/V_{\text{day}=1}$) as a function of days after thermal neutron beam irradiation [$N = 5$, $p^* < 0.05$ from Gd-DO3A-BTA(+), n-]. Adapted and reproduced with permission from ref 11j. Photograph courtesy of Ki-Hye Jung. Copyright 2018 Ki-Hye Jung et al.

Gd in human sarcoma malignant fibrosis histiocytoma (MFH) Nara-H cells, compared to that (9.5 μg Gd) obtained with Gd-DTPA.^{12b} Tokumitsu et al. observed a higher accumulation and longer retention of Gd-nanoCPs ($a = 425$ nm) in cancer after intratumoral injection into B16F10 cancer-bearing mice, compared to those obtained with Gd-DTPA (Figure 6b).^{12c} As

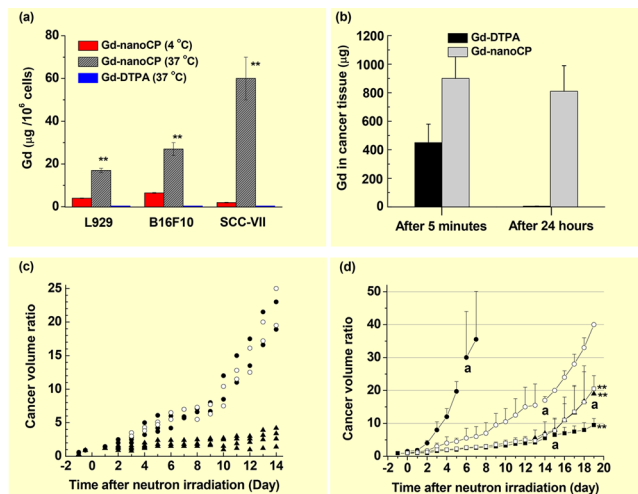


Figure 6. (a) Histograms of Gd-accumulation concentrations: Gd-nanoCPs ($d = 426$ nm) at 4 and 37 °C, and Gd-DTPA at 37 °C in three types of cells (L929, B16F10, and SCC-VII), 12 h after incubation and washing out of free Gd-nanoCPs and Gd-DTPA from the cells with a PBS solution ($n = 3$, $p^{**} < 0.001$ from the values at 4 °C). Reproduced with permission from ref 12a. Copyright 2002 Elsevier. (b) Histograms of Gd-accumulation concentration of Gd-nanoCPs ($d = 425$ nm) and Gd-DTPA in cancer, 5 min and 24 h after intratumoral injection into B16F10 cancer-bearing mice. Reproduced with permission from ref 12c. Copyright 1999 Plenum Publishing Corporation. (c) Plots of cancer-volume suppression ratios ($V_{\text{day}}/V_{\text{day}=0}$) of B16F10 cancer-bearing mice as a function of days after thermal neutron beam irradiation: no Gd (○) ($N = 2$), Gd-DTPA (●) ($N = 2$), and Gd-nanoCP (▲) ($N = 4$). Reproduced with permission from ref 12d. Copyright 2000 Elsevier. (d) Plots of cancer-volume suppression ratios ($V_{\text{day}}/V_{\text{day}=0}$) of B16F10 cancer-bearing mice as a function of days after thermal neutron beam irradiation: cold control (●) (no injection, n-), hot control (○) (saline, n+), Gd-nanoCP-400 (▲) (2.4 mg Gd, n+), Gd-nanoCP-200 (■) (2.4 mg Gd, n+), Gd-nanoCP-200 (□) (1.2 mg Gd, n+) ($N = 5-6$, $p^{**} < 0.01$ from hot control group). Labels "a" indicate the time point at which death of a mouse was observed. Reproduced with permission from ref 12e. Copyright 2013 Elsevier.

shown, Gd-DTPA was rapidly excreted from cancer, while ~90% of Gd-nanoCPs remained in the cancer cells up to 24 h after injection. In addition, they performed *in vivo* GdNCT experiments on B16F10 cancer-bearing mice after intratumoral injection with Gd-nanoCPs ($a = 430$ nm) by irradiating thermal neutrons 8 h after injection. They observed a significant cancer-growth suppression after irradiation, while the mice injected with Gd-DTPA exhibited minor suppression after irradiation (Figure 6c).^{12d} This was due to a higher accumulation of Gd-nanoCPs, compared to that of Gd-DTPA.^{12c} Ichikawa et al. applied Gd-nanoCP-400 ($a = 391$ nm) and Gd-nanoCP-200 ($a = 214$ nm) in GdNCT on B16F10 cancer-bearing mice.^{12e} They observed a higher accumulation of Gd-nanoCP-200 (~1500 μg Gd/g cancer tissue) than that of Gd-nanoCP-400 (~600 μg Gd/g cancer tissue) 8 h after intratumoral injection with the same dose of 2.4 mg Gd/mouse. Consequently, an enhanced cancer-growth suppression was observed with Gd-nanoCP-200 (Figure 6d). This result was attributed to a higher and more homogeneous accumulation of Gd-nanoCP-200, compared to that of Gd-nanoCP-400, owing to the smallness of Gd-nanoCP-200.

3.3.2. Polyamidoamine (PAMAM) Nanocomposites. Dendrimers such as PAMAM, a well-defined hyperbranched

spherical polymer,^{21c} have been applied as nanocarriers in the delivery of a large amount of Gd-chelates to cancer cells. PAMAM is highly water-soluble and contains numerous primary amine groups on its surface, which are useful in incorporating Gd-chelates through amide bonds. PAMAMs are classified into various generations according to the number of primary amines on their surfaces. For example, the first generation PAMAM (G_1 -PAMAM) contains 8 primary amines on its surface, while the sixth generation PAMAM (G_6 -PAMAM) has 256 primary amines on its surface.^{21c} Kobayashi et al. employed G_6 -PAMAM to synthesize 2 types of nanocomposites: G_6 Gd in which Gd-DTPAs were attached to G_6 -PAMAM and avidin- G_6 Gd in which both Gd-DTPAs and avidins were attached to G_6 -PAMAM.^{13a} Avidin can target human ovarian cancer (SHIN3) cells.^{21d} They measured Gd-concentration in cancer *in vitro* and *in vivo*. Owing to avidin, the accumulation of avidin- G_6 Gd in SHIN3 cells was 3.5 times higher than that of G_6 Gd and 50 times higher than that of Gd-DTPA in *in vitro* cell culture experiments. For *in vivo* experiments, the accumulation of avidin- G_6 Gd in SHIN3 cells (162 ppm Gd or 25.4 ppm ^{157}Gd) was 3.4 times higher than that of G_6 Gd and 366 times higher than that of Gd-DTPA 1 day after intraperitoneal injection into SHIN3 cancer-bearing mice. This accumulated avidin- G_6 Gd in SHIN3 cells was close to the optimal ^{157}Gd -concentration for GdNCT experiments (50–200 ppm ^{157}Gd in cancer).^{15a} Thus, it will be useful for GdNCT applications.

3.3.3. Poly(Amino Acid) Nanocomposites. Poly(amino acids) have attracted significant interest because they can be used as drug nanocarriers, owing to their good biocompatibility and biodegradability.^{21e} Monomers in poly(amino acids) contain functional groups, such as carboxyl, amino, hydroxyl, and thiol groups, which can be conjugated to other functional molecules, such as drugs and cancer-targeting ligands.^{21e} Among poly(amino acids), poly(aspartic acid) has been used in hydrogel synthesis and other biomedical applications.^{21f} Qin et al. conjugated poly(aspartic acid) ($M_w = \sim 25$ kDa) with two kinds of poly(ethylene glycol) (PEG) [$M_w = \sim 12$ kDa (PEG₂₇₂) and ~ 20 kDa (PEG₄₅₄)] through amide bonds to synthesize P272 and P454 nanocomposites with $a = 8.3$ and 9.8 nm, respectively.^{13b} The nanocomposites were further grafted with 33–38 Gd-DOTA-NH₂ through amide bonds, respectively. PEG conjugation (PEGylation) is generally used to increase the solubility, stability, and blood circulation half-life of drugs.^{21g} Additionally, it is used to reduce their uptake by the reticuloendothelial system to enhance therapeutic efficacy.^{21g} The *in vitro* cellular uptake of P272 (2.1 nM Gd/10⁶ cells) in murine colon adenocarcinoma 26 (C-26) cells 24 h after incubation was two times higher than that (1.1 nM Gd/10⁶ cells) of P454.^{13b} For *in vivo* experiments on C-26 cancer-bearing mice, P454 exhibited an ~ 2 times higher Gd-accumulation than P272 in cancer, 8 h after the intravenous injection of 10 mg Gd/kg. These results were attributed to a higher enhanced permeability and retention (EPR) effect^{21h} of P454, compared to P272. For *in vivo* GdNCT experiments, 0.2 mL of P272, P454, Gd-DTPA, and saline solutions were intravenously injected into mice (injection dose = 30 mg Gd/kg). The mouse groups injected with P272 and P454 exhibited higher cancer-growth suppression than those obtained with Gd-DTPA and saline solutions after thermal neutron beam irradiation (Figure 7). The saline-solution mouse group showed similar anticancer activity as the Gd-DTPA mouse group because Gd-DTPA was rapidly excreted via the renal

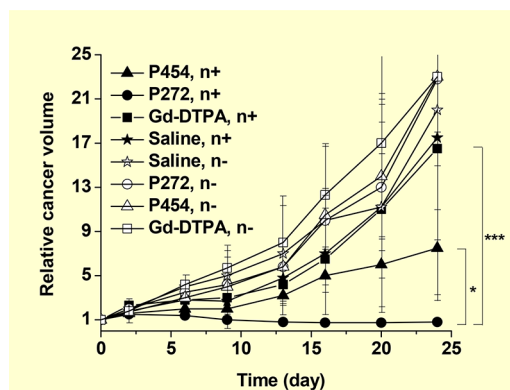


Figure 7. Plots of relative cancer volume ($V_{\text{day}}/V_{\text{day}=0}$) as a function of days after thermal neutron beam irradiation ($N = 3$, $p^* < 0.05$, $p^{***} < 0.001$). Reproduced with permission from ref 13b. Copyright 2020 Wiley-VCH.

system within a few hours^{20a} after injection. All the nonirradiated mouse groups exhibited negligible anticancer activity, implying no *in vivo* toxicity in P272 and P454. The P272 mouse group exhibited a higher GdNCT effect than the P454 mouse group despite the higher Gd-accumulation of P454. They attributed this to a better penetration of small P272 in the cancer cells, compared to that of P454, such that highly ionizing ACK and IC electrons could effectively contribute to cancer-cell death. This indicated that among particles produced from the thermal NC reaction of ^{157}Gd and ^{155}Gd , ACK and IC electrons were more effective than γ -rays in killing cancer cells.

3.3.4. Cellulose Microcapsules. Ethylcellulose, a non-biodegradable and biocompatible polymer, has been extensively studied in the encapsulation of drugs.²¹ⁱ Akine et al. encapsulated Gd-DTPA in ethylcellulose microcapsules and applied them to the *in vivo* GdNCT of Ehrlich ascites cancer-bearing mice.^{13c} The microcapsules had $a = 75$ – 106 μm , and the weight% of Gd-DTPA was 31%. The microcapsules slowly released Gd-DTPA in solution, allowing an extended retention of Gd-DTPA in the microcapsules. The cancer model mice were prepared by intraperitoneally injecting $\sim 10^7$ Ehrlich ascites cancer cells into mice. Afterward, 220 mg of the microcapsules suspended in 0.5 mL of a dextran-40 solution were intraperitoneally injected into mice, and a thermal neutron beam was irradiated onto their anterior abdomens within 5 min after injection. The ^{157}Gd -concentration 17 min after injection was approximately 2.5 mg $^{157}\text{Gd}/\text{mL}$ of the peritoneal fluid. The result showed that approximately 32% of the (Gd+, n+) mouse group survived up to 60 days after irradiation, whereas 100% of the (Gd-, n+), (Gd+, n-), and (Gd-, n-) mouse groups survived less than 18 days after irradiation, demonstrating GdNCT effects. Owing to the extracellular properties of the microcapsules and Gd-DTPA, the GdNCT effects were mainly due to the γ -rays and high-energy (>20 keV) IC electrons, not the low-energy ACK and IC electrons.

3.3.5. Calcium Phosphate Nanocomposites. Calcium phosphate (CaP) is found in many parts of the human body, such as bone mineral and tooth enamel, and has been considered a potential drug nanocarrier because of its biocompatibility, biodegradability, and low cost.^{21j} Mi et al. modified CaP with PEG-block-poly(aspartic acid) [PEG-*b*-P(Asp)] to prepare hybrid micelles, in which Gd-DTPA were

incorporated.^{14a} They applied the Gd-DTPA/CaP nanocomposites ($a = \sim 55$ nm) to *in vitro* and *in vivo* GdNCT experiments. The *in vitro* GdNCT experiments with 100 μ M Gd of Gd-DTPA/CaP nanocomposites and Gd-DTPA without washing C-26 cancer cells after incubation exhibited similar GdNCT effects with approximately 50% cancer-cell viabilities probably due to extracellular properties of nanocomposites and Gd-DTPA. For *in vivo* experiments with an injection dose of 0.02 mmol Gd/kg in C-26 cancer-bearing mice, a higher Gd-accumulation of Gd-DTPA/CaP nanocomposites [3.9% of the injected dose estimated from inductively coupled plasma atomic emission spectroscopy (ICP-AES)] in the cancer cells, compared to that of Gd-DTPA was obtained, owing to the EPR effect^{21h} of the nanocomposites, 10 h after intravenous injection. This higher Gd-accumulation of the nanocomposites was confirmed in the MR images (Figure 8a and b) and tumor-to-normal tissue contrast ratios (Figure 8c). The *in vivo* GdNCT experiments with Gd-DTPA/CaP nanocomposites (intravenous injection dose = 0.05 mmol Gd/kg) exhibited the lowest cancer-volume enhancement with time among four

mouse groups (Figure 8d) and a 5-fold smaller cancer volume than that obtained with Gd-DTPA, 27 days after thermal neutron beam irradiation (Figure 8d and e). Dewi et al. reported a higher Gd-accumulation in cancer after three-time intravenous injection of Gd-DTPA/CaP nanocomposites ($a = \sim 60$ nm) into C-26 cancer-bearing mice, compared to that obtained with a single injection.^{14b} However, the cancer-volume suppression of the three-time injection case was similar to that of the single-injection case (Figure 8f). This was attributed to the enhanced depression of the thermal neutron beam intensity by extra Gd-DTPA/CaP nanocomposites accumulated in superficial cancer cells, such that the deeper part of the cancer was less irradiated in three-time injection case.

3.3.6. Liposome Nanocomposites. Liposomes are vesicles made of lipid bilayer membranes capable of entrapping a large amount of drugs. Consequently, they have been studied for decades as drug delivery systems.^{21k} Several drugs encapsulated inside liposomes, such as DaunoXome and Doxil, are now commercially available for clinical use.^{21k}

Le and Cui prepared liposomes using soy-hydrogenated-phosphatidylcholine, cholesterol, and 1,2-distearoyl-*sn*-glycero-3-phosphoethanolamine-*N*-[methoxy(polyethylene glycol)-2000] and applied them to the delivery of Gd-DTPA to cancer *in vivo*.^{15a} The Gd-DTPA-encapsulated liposomes were intravenously injected into subcutaneous human cervical (TC-1) cancer-bearing mice with an injection dose of 414 μ g Gd/mouse. This injection dose resulted in an uptake of 158.9 ± 43.7 μ g Gd/g cancer tissue, 12 h after injection. With a triple-injection dose, the Gd-concentration increased to 233.9 ± 81.2 μ g Gd/g cancer tissue. These corresponded to 24.9 and 36.7 ¹⁵⁷Gd/g cancer tissue, respectively, which were relatively close to the required ¹⁵⁷Gd-amount for GdNCT experiments (50–200 μ g ¹⁵⁷Gd/g cancer tissue).^{15a} This study showed that liposomes are potential nanocarriers and can deliver a large amount of Gd to cancer via multiple injections, which would be useful in GdNCT applications.

Dewi et al. used a nonionic Coatsome EL-01-N liposome ($a = 100$ – 300 nm), which comprised dipalmitoylphosphatidylcholine, cholesterol, and dipalmitoylphosphatidylglycerol to encapsulate Gadoteridol (Gd-HP-DO3A, Figure 3g) for *in vivo* GdNCT experiments.^{15b} First, 2.0 mL of 0.5 M Gadoteridol was poured into a vial containing the Coatsome EL-01-N. The liposome nanocomposite solution was intravenously injected into the tail veins of C-26 cancer-bearing mice with an injection dose of 0.2 mL (0.1 mmol Gd)/mouse. This injection dose led to a maximum accumulation of 40.3 μ g Gd/g cancer tissue, 2 h after injection, which decreased by half, 12 h after injection. However, with Gadoteridol, the accumulation was only 0.046 μ g Gd/g cancer tissue, 2 h after injection. The liposome nanocomposites showed a significant anticancer effect such that 27 days after thermal neutron beam irradiation, the cancer volume of the (Gd+, n+) mouse group was the smallest among the mouse groups (Figure 9a) and four times less than that of the (Gd–, n–) control mouse group (Figure 9b).

The cellular uptake of liposome nanocomposites and the resulting GdNCT effect depend on the liposome composition. This was confirmed by Peters et al. when they synthesized five kinds of liposomes: 1,2-dioleoyl-*sn*-glycero-3-phosphocholine (DOPC)–cholesterol (Chol)–1,2-dioleoyl-3-trimethylammonium-propane (DOTAP), DOPC–Chol–cardiolipin (CL), DOPC–Chol–1,2-dioleoyl-*sn*-glycero-phosphoethanolamine

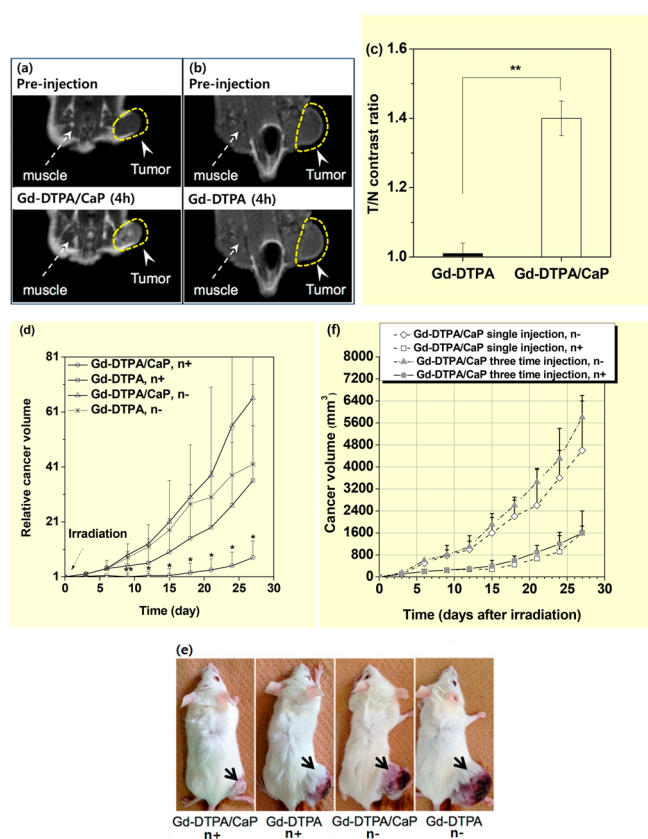


Figure 8. T₁-weighted MR images before and 4 h after intravenous injection of (a) Gd-DTPA/CaP nanocomposites and (b) Gd-DTPA. (c) Tumor-to-normal (T/N) tissue contrast ratios estimated from T₁-weighted MR images in a and b ($N = 3$, $p^{**} < 0.01$). (d) Relative cancer volume ($V_{\text{day}}/V_{\text{day}=0}$) of four C-26 cancer-bearing mouse groups as a function of days with and without thermal neutron beam irradiation ($N = 4$ – 5 , $p^{**} < 0.01$, $*p < 0.05$ from other groups). (e) Photographs of C-26 cancer-bearing mice taken on day 27 after thermal neutron beam irradiation. Adapted and reproduced from ref 14a. Copyright 2015 American Chemical Society. (f) Cancer volume of four C-26 cancer-bearing mouse groups as a function of days after thermal neutron beam irradiation. Reproduced with permission from ref 14b. Photograph courtesy of N. Dewi. Copyright 2016 Springer.

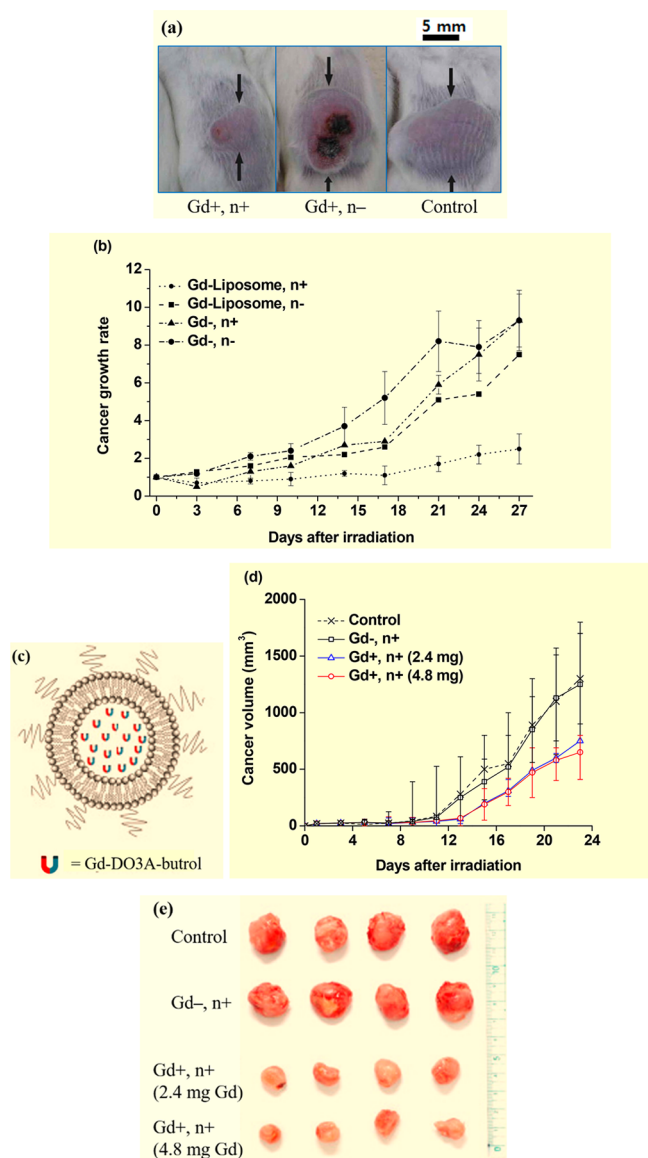


Figure 9. (a) Photographs of three mouse groups 27 days after thermal neutron beam irradiation, showing the smallest cancer volume for the (Gd+, n+) mouse group. (b) Normalized cancer volume ($V_{\text{day}}/V_{\text{day}=0}$) of four mouse groups as a function of days after thermal neutron beam irradiation. Adapted and reproduced with permission from ref 15b. Copyright 2013 Elsevier. (c) PEGylated liposome containing Gd-DO3A-butrols. (d) Plots of cancer volumes of the four mouse groups as a function of days after irradiation ($N = 4$): (Gd-, n-) control, (Gd-, n+), (Gd+, n+) (2.4 mg Gd/mouse), and (Gd+, n+) (4.8 mg Gd/mouse). (e) Photographs of cancers resected from mice 23 days after irradiation. Adapted and reproduced with permission from ref 15d. Photograph courtesy of W. Lee. Copyright 2021 Elsevier.

(DOPE), DOPC–Chol–folate(polyethylene glycol) (Fol-PEG), and DOPC–DOPE with diameters ranging from 136 to 152 nm.^{15c} They were used to encapsulate Gd-DTPA for cellular uptake and *in vitro* GdNCT experiments. Rat glioma (F98) and human glioblastoma (LN229) cells were incubated with liposome nanocomposites and Gd-DTPA. All the liposome nanocomposites showed higher cellular uptakes than those obtained with Gd-DTPA after washing out the free liposome nanocomposites and Gd-DTPA from the cells with a PBS solution. Notably, liposome composition-depend-

ent Gd-concentrations in cells were observed. Additionally, 97 h after thermal neutron beam irradiation, the cell viability assay showed that the DOPC–DOPE, DOPC–Chol–FolPEG, and DOPC–Chol–DOTAP liposome nanocomposites were the most effective Gd-formulations to deactivate the F98 and LN229 glioma cells. These cellular uptakes and *in vitro* GdNCT results implied that a proper choice of liposome composition could enhance the intracellular Gd-concentration and consequently the GdNCT result.

Most recently, Lee et al. synthesized PEGylated liposomes using 1,2-dipalmitoyl-*sn*-glycero-3-phosphocholine, 1,2-dihexadecanoyl-*sn*-glycero-3-phospho-(1'-rac-glycerol), cholesterol, and 1,2-distearoyl-*sn*-glycero-3-phosphoethanolamine-*N*-[methoxy(polyethylene glycol)-2000] (Figure 9c) and applied them to the delivery of Gd-DO3A-butrol to cancer *in vivo*.^{15d} The PEGylated liposome ($a = 96.7$ nm) solution was intravenously injected into the tails of CT26 cancer-bearing mice with injection doses of 2.4 and 4.8 mg Gd/mouse, 20 min before thermal neutron beam irradiation. They observed considerable cancer-growth suppression in the (Gd+, n+) GdNCT group, compared to that of the (Gd-, n-) control group; the cancer volume of the GdNCT group was 43% of the control group 23 days after irradiation for 2.4 mg Gd/mouse injection dose case (Figure 9d). Photographs of cancers resected from the mice 23 days after irradiation clearly demonstrated cancer-volume suppressions from the control group (Figure 9e). The mouse group with 4.8 mg Gd/mouse injection dose exhibited a better cancer-growth suppression, compared to that of the mouse group with 2.4 mg Gd/mouse injection dose (Figure 9d), but the improvement was small, probably because a low neutron fluence (1.4×10^7 neutrons cm^{-2}) was used (the typical value^{13b,14a} is $\sim 10^{12}$ neutrons cm^{-2}). Additional injections and irradiation 10 days after the first irradiation led to improved cancer-growth suppressions for both injection doses; for the 2.4 mg Gd/mouse injection dose case, the cancer volume was 30% of the control group 31 days after the first irradiation.

3.4. Gd Metallofullerene Nanoparticles. Horiguchi et al. used Gd metallofullerenes in which one Gd atom was contained in a C_{82} fullerene cage (80–90% purity of $\text{Gd}@\text{C}_{82}$; the remaining ones contained $\text{Gd}@\text{C}_{80}$, $\text{Gd}_2@\text{C}_{78}$, and $\text{Gd}_2@\text{C}_{80}$) as a GdNCT agent *in vitro*.¹⁶ They were produced via the arc-heating of a Gd_2O_3 /graphite composite rod as a positive electrode (anode).^{22a} The $\text{Gd}@\text{C}_{82}$ nanoparticles were solubilized in water via a complex formation (not a covalent bond) with a biocompatible synthetic block copolymer, poly(ethylene glycol)-*b*-poly(*N,N*-(dimethylamino)ethyl methacrylate) (PEG-*b*-PAMA) through the sonification of $\text{Gd}@\text{C}_{82}$ nanoparticles and PEG-*b*-PAMA in dimethylformamide (Figure 10a). The synthesized $\text{Gd}@\text{C}_{82}$ -PEG-*b*-PAMA nanoparticles showed $a = 20$ –30 nm and extremely low cytotoxicity against C-26 cancer cells up to 634 μM Gd. The C-26 cancer cells were cultured with $\text{Gd}@\text{C}_{82}$ -PEG-*b*-PAMA nanoparticles at Gd-concentrations of 10 (63.4 μM), 50 (317 μM), and 100 ppm Gd (634 μM Gd) for 30 min, and thermal and epithermal neutron beams were irradiated without washing out the free nanoparticles. The cancer cells incubated at 0 (control) and 10 ppm Gd did not show cancer-cell death, regardless of irradiation, probably because the Gd-concentration was less than the required Gd-concentration for cancer-cell death in GdNCT. The latter two Gd-concentrations showed cancer-cell death, which increased with increasing Gd-concentration, exhibiting GdNCT effects (Figure 10b).

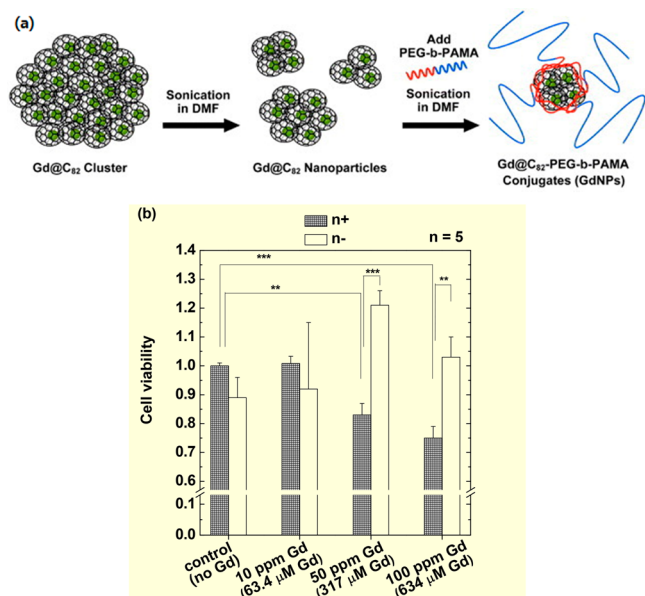


Figure 10. (a) Preparation of Gd@C₈₂-PEG-b-PAMA nanoparticles. (b) Cell viability of C-26 cells before (white bars) and after (meshed bars) neutron beam irradiation in the absence (control) and presence of Gd@C₈₂-PEG-b-PAMA nanoparticles at various Gd-concentrations ($n = 5$, $p^{**} < 0.05$, $p^{***} < 0.001$). Adapted and reproduced with permission from ref 16. Copyright 2011 National Institute for Materials Science.

Unirradiated cancer did not show cancer-cell deaths, indicating that the nanoparticles themselves were not toxic.

3.5. Solid-State Nanoparticles. Solid-state nanoparticles are compact and can deliver a significantly large amount of Gd to cancer. Four kinds of solid-state Gd-nanoparticles have been applied in *in vitro* and *in vivo* GdNCT experiments,^{17a–d} as described below.

3.5.1. Gd-Doped Cobalt/Carbon Core–Shell Nanoparticles (GdCo@CNPs) (Core = Gd-Doped Cobalt Nanoparticle and Shell = Carbon). Hwang et al. synthesized Gd-doped cobalt/carbon core–shell nanoparticles (GdCo@CNPs) through a pulsed direct current arc-discharge method [anode = graphite electrode filled with Gd oxide/cobalt oxide (1:1 mol ratio); cathode = tungsten] and applied them in *in vitro* GdNCT.^{17a} The particle diameters measured with a transmission electron microscope (TEM) ranged from 20 to 50 nm. The GdCo@CNPs were surface-modified with poly(acrylic acid) (PAA) for water solubility and conjugated with NH₂-polyoxyethylene (PEG)-folate to allow the nanoparticles to bind to folate receptors, which were overexpressed on HeLa cancer-cell membranes. This conjugation was aimed at increasing the nanoparticle uptake by the cancer cells via receptor-mediated endocytosis.^{22b} After 24 h of incubating HeLa cells with 0.09677 μg GdCo@CNPs (4.4 mol % of Gd), the incubated cells were washed out with a PBS solution twice to remove free nanoparticles and irradiated with a thermal neutron beam. Notably, 55% of the irradiated HeLa cells after normalization with respect to the irradiated control cells with no Gd were dead, 8 h after irradiation (Figure 11a). As shown, they also attempted to use BCo@CNPs (52% cancer-cell death) and Co@CNPs (28% cancer-cell death) (⁵⁹Co, $\sigma = 1900$ barns,² 100% natural abundance) as GdNCT agents. Therefore, the GdCo@CNPs exhibited the highest cancer-cell killing among the three nanoparticle types. As observed,⁵⁹Co

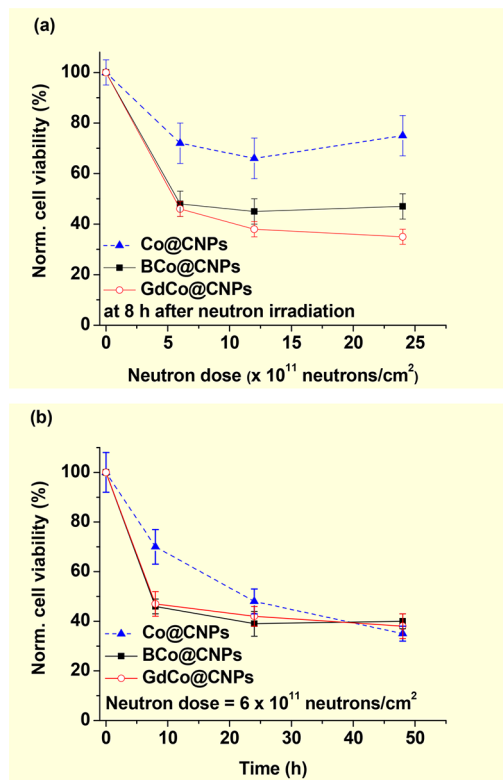


Figure 11. (a) Normalized HeLa cell viabilities as a function of the thermal neutron irradiation dose at 8 h after neutron beam irradiation. The HeLa cells were incubated with different M@CNP nanoparticles (M = Co, BCo, and GdCo) and washed out with a PBS solution. (b) Normalized HeLa cell viabilities as a function of hours after thermal neutron beam irradiation at a neutron beam dose of 6×10^{11} neutrons/cm². All cell viabilities were normalized using the control cells, which were not incubated with nanoparticles but received thermal neutrons. Reproduced with permission from ref 17a. Copyright 2010 Elsevier.

was converted into radioactive ⁶⁰Co (half-life = 5.26 years) after the absorption of neutrons.^{22c} Thus, the Co@CNPs exhibited a long-term cancer-cell killing effect, as shown in Figure 11b. Radioactive elements are harmful to the body and thus not suitable for use in NCT agents. However, they are not produced from ¹⁵⁷Gd, ¹⁵⁵Gd, and ¹⁰B. Therefore, Gd and B isotopes can be safely used in NCT agents.

3.5.2. PEG-Silica@Gd₂O₃ Nanoparticles. Bridot et al. synthesized Gd oxide (Gd₂O₃) nanoparticles through a polyol method.^{17b} They were subsequently embedded in a polysiloxane shell and grafted with PEG(COOH)₂. The core–shell nanoparticles (core = Gd₂O₃ nanoparticle; shell = PEG-silica) with extremely small hydrodynamic diameters of ~3.3 nm were applied in *in vitro* GdNCT. The mouse lymphoma cancer cells transfected by luciferase coding gene (EL4-LUC cells) were used as cancer cells because only the live cells could exhibit fluorescence via luciferase bioactivity, after thermal neutron beam irradiation. The cancer cells were incubated with the nanoparticles at various Gd-concentrations (0.01, 0.05, 0.10, and 0.30 mM Gd) for 30 min and thoroughly washed with a buffer solution to remove free nanoparticles. The cells exhibited an uptake saturation concentration of ~14 pg Gd/cell above ~0.1 mM Gd-incubation concentration. The nanoparticles alone up to 0.3 mM Gd and the thermal neutron beam alone up to 3.0 Gy were harmless to the cells;

however, cell death was observed at a 7.0 Gy thermal neutron beam dose. This cell death at high neutron beam dose was due to the thermal neutron beam absorption by cell elements (C, H, O, and N) with tiny σ values,² as commonly observed in GdNCT experiments.^{11a–c,g,17d} Therefore, they conducted *in vitro* GdNCT experiments within 1.0–3.0 Gy thermal neutron beam irradiation doses for 0.0–0.3 mM Gd-incubation concentrations. They observed that cell death increased with an increase in the neutron beam irradiation dose and Gd-incubation concentration. From the results, the authors suggested that for efficient EL4-LUC cell killing, the neutron beam dose should be 3.0 Gy and Gd-incubation concentration should exceed 0.05 mM Gd.

3.5.3. Rho-PAA-Coated Gd_2O_3 Nanoparticles. The application of gadolinium oxide nanoparticles in multifunctional MRI and therapy has increased.²³ A recent report by Ho et al. on the synthesis of Gd_2O_3 nanoparticles coated using PAA and rhodamine (Rho) (Gd_2O_3 -PAA-Rho) resulted in ultrasmall nanoparticles (average particle diameter = ~ 1.5 nm) with high colloidal stability in aqueous media (Figure 12a).^{17c} They applied the Gd_2O_3 -PAA-Rho nanoparticles in *in vitro* GdNCT experiments on human brain malignant glioblastoma (U87MG) cells, dual-modal MRI, and pH-sensitive fluorescent cancer-cell detection. The cells were incubated with Gd_2O_3 -PAA-Rho nanoparticles and commercial Gadovist at the same Gd-concentration of 0.5 mM Gd for 24 h and washed out with a PBS solution three times to remove free nanoparticles and Gadovist from the cells. *In vitro* GdNCT experiments were performed for two sets of cell numbers (500 and 1000), including control cells with no Gd (Figure 12b). Thermal neutron beam irradiation of ~ 6 Gy led to 28.1% more average cancer-cell death, compared to that of the control cells, which received only irradiation with no Gd (Figure 12c). Additionally, this cancer-cell death was 1.75 times higher than that obtained with Gadovist (Figure 12c).

3.5.4. RGD-PAA-Coated Gd_2O_3 Nanoparticles. Nanoparticles conjugated with cancer-targeting ligands can enhance cellular uptake in cancer cells through active targeting with cancer-targeting ligands²⁴ and passive targeting via EPR effects.^{21h} Recently, Ho et al. conjugated $-COOH$ groups of PAA-coated Gd_2O_3 nanoparticles (average particle diameter = 1.8 nm) with $-NH_2$ groups of linear arginyl glycol aspartic acid (RGD) as a cancer-targeting ligand and applied Gd_2O_3 -PAA-RGD nanoparticles in *in vivo* GdNCT experiments on subcutaneous U87MG cancer-bearing mice.^{17d} From T_1 MR images, the maximal Gd-accumulation time of Gd_2O_3 -PAA-RGD nanoparticles was determined to be ~ 20 min after the intravenous injection of 0.1 mmol Gd/kg into a mouse tail. The maximal Gd-accumulation amount was estimated to be $2.2 \mu\text{g Gd/g}$ cancer tissue via ICP-AES after sacrificing the mouse. This value was less than the optimal ^{157}Gd -amount for GdNCT ($50\text{--}200 \mu\text{g } ^{157}\text{Gd/g}$),^{15a} indicating a low cancer-targeting performance by the nanoparticles probably because 3–4 RGDs were conjugated per nanoparticle. Therefore, more RGDs should be conjugated per nanoparticle to increase Gd-accumulation in cancer through active targeting. As shown in the photographs and T_1 MR images (Figure 13a), the (Gd+, n+) mouse group showed a considerably smaller cancer volume, compared to that of the (Gd–, n–) control mouse group. The V/V_0 of the (Gd+, n+) mouse group in which V_0 and V are the cancer volumes before and after thermal neutron beam irradiation, respectively, was eight times smaller than that of the control mouse group 25 days after irradiation (Figure 13b

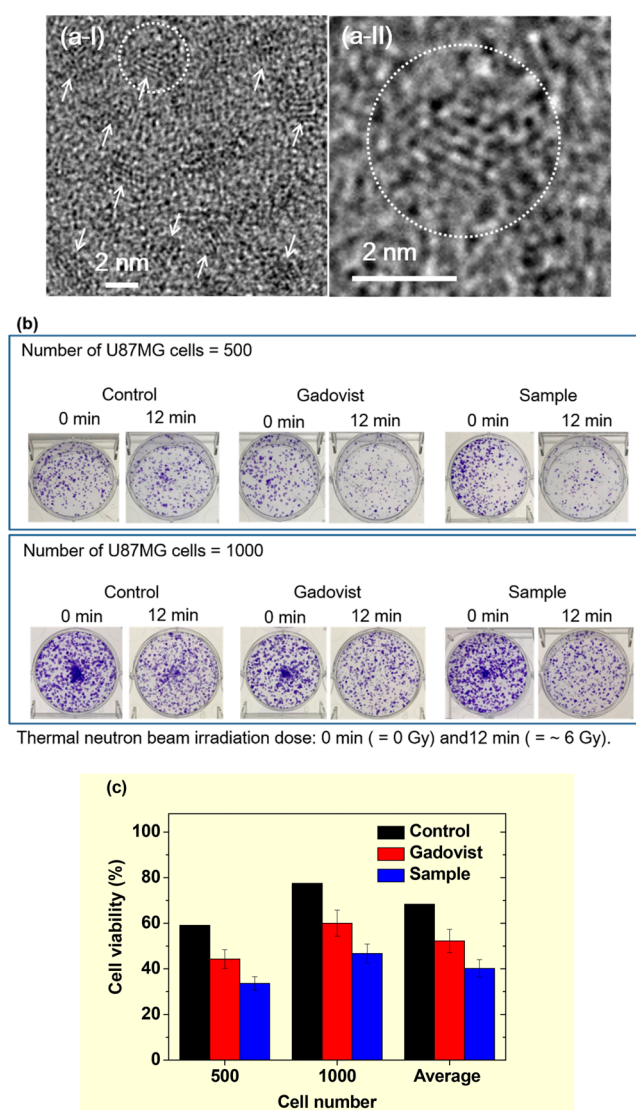


Figure 12. (a) (I)–(II) High-resolution TEM images at different magnifications [arrows in (a-I) indicate ultrasmall Rho-PAA-coated Gd_2O_3 nanoparticles, and the circled region in (a-I) was magnified in (a-II)]. (b) Photographs of six sets of cell dishes containing U87MG cancer cells with 500 (top) and 1000 (bottom) cell numbers 2 weeks after colonial formation. 0 and 12 min indicate no and ~ 6.0 Gy thermal neutron beam irradiation, respectively. (c) Histograms of cell viabilities of irradiated U87MG cancer cells after normalization using those of the corresponding unirradiated cells. In (b) and (c), labels indicate control (no Gd), Gadovist (0.5 mM Gd), and sample (nanoparticle, 0.5 mM Gd). Adapted and reproduced with permission from ref 17c. Photograph courtesy of S. L. Ho and K.-H. Jung. Copyright 2018 The Royal Society of Chemistry.

and c). The slight cancer-growth suppression of the (Gd+, n–) mouse group, compared to that of the control mouse group was attributed to a slight toxicity in the nanoparticles to U87MG cells, as observed in *in vitro* cellular cytotoxicity measurements of the nanoparticles.^{17d} In addition, the slight cancer-growth suppression of the (Gd–, n+) group was due to tiny thermal neutron beam absorptions by cell elements (^1H , ^{12}C , ^{14}N , and ^{16}O),² as commonly observed in GdNCT experiments.^{11a–c,g,17b} However, the thermal neutron beam alone at low doses was not harmful to cancer cells,^{17b} implying

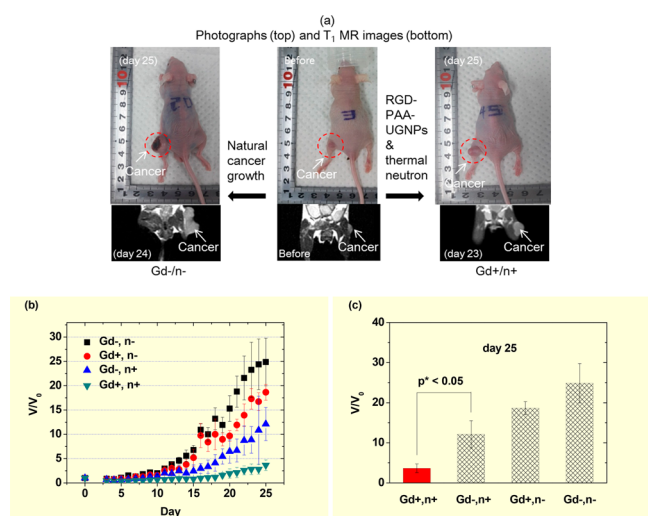


Figure 13. (a) Photographs (top) and T₁ MR images (bottom) of (Gd-, n-) (left), (Gd-, n-) (middle), and (Gd+, n+) (right) mice 24, 0, and 23 days after thermal neutron beam irradiation, respectively. (b) Plots of V/V₀ (V₀, cancer volume prior to irradiation) as a function of days after thermal neutron beam irradiation (N = 5). (c) Plots of V/V₀ of the four mouse groups 25 days after the thermal neutron beam irradiation (N = 5, p* < 0.05). Adapted and reproduced with permission from ref 17d. Photograph courtesy of S. L. Ho and G. Choi. Copyright 2020 The Royal Society of Chemistry.

that a low neutron beam dose is preferred for GdNCT as long as it is effective.

4. PERFORMANCE COMPARISON STUDIES WITH BNCT

Several comparison studies with BNCT have been conducted.^{11d,i,17a} Tokuyue et al. observed a higher Chinese hamster V79 cell death in *in vitro* cellular NCT experiments using Gd-DTPA than that obtained with BSH (Figure 4f).^{11d} Mitin et al. observed that Na₂(Gd-DTPA) was more effective in interstitial osteosarcoma, compared to BPA in *in vivo* NCT experiments on dogs.¹¹ⁱ Hwang et al. observed slightly higher HeLa cancer-cell deaths in *in vitro* cellular NCT experiments using GdCo@CNPs, compared to those obtained with BCo@CNPs (Figure 11a).^{17a} All comparison studies suggest that GdNCT is better than BNCT. This is probably because ¹⁵⁷Gd and ¹⁵⁵Gd generate more particles to kill cancer cells (5 ACK electrons, 0.69 IC electrons, and 1.8 γ -rays), compared to ¹⁰B which generates one α and one ⁷Li.^{2,7} In addition, σ values of ¹⁵⁷Gd and ¹⁵⁵Gd are 66 and 15.8 times higher than that of ¹⁰B, respectively;^{2,7} this further makes more particles generated in

¹⁵⁷Gd and ¹⁵⁵Gd, compared to ¹⁰B. The number of particles generated per isotope, assuming the linearity to σ and natural abundance [15.7% (¹⁵⁷Gd), 14.8% (¹⁵⁵Gd), and 19.9% (¹⁰B)] and after normalization with respect to ¹⁰B, is provided in Table 3. 478.0 particles are generated from both ¹⁵⁷Gd and ¹⁵⁵Gd, while 2.0 particles are generated from ¹⁰B. Considering the relative biological effectiveness (RBE) weighting factor,²⁵ the RBE weighting factor-weighted number of particles are 478.0 (¹⁵⁷Gd and ¹⁵⁵Gd) and 40.0 (¹⁰B); this estimation suggests that GdNCT is approximately 10 times more powerful than BNCT.

In particular, five ACK electrons are generated per Gd, while 0.69 IC electrons and 1.8 γ -rays are generated per Gd. Therefore, their contribution to cancer-cell killing will be more significant, compared to those of IC electrons and γ -rays. For γ -rays, this was confirmed in experiments on SW-1573 cancer cells using Gd-DTPA^{11c} and C-26 cancer-bearing mice using polymeric nanocomposites containing Gd-DOTA.^{13b} This implies that intracellular GdNCT agents will be powerful in NCT because they can penetrate cancer cells, and consequently, many ACK electrons can be generated near cancer-cell DNAs and then participate in cancer-cell killing.

5. MRI-GUIDED GDNCT

It is noteworthy that GdNCT agents can serve as theranostic (or MRI-guided GdNCT) cancer agents because Gd can be used as MRI contrast agents.⁹ In MRI-guided GdNCT experiments, cancer size, shape, and position can be diagnosed *via* MRI before and after NCT (currently available) or on real time during NCT (currently not available) (Figure 14). In the

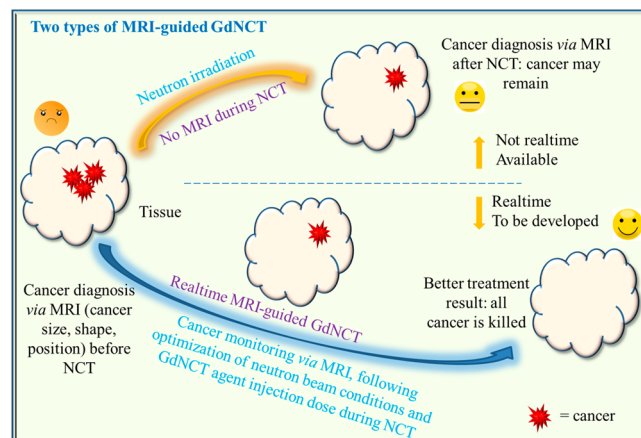


Figure 14. Two types of MRI-guided GdNCT. Cancer monitoring *via* MRI before and after NCT (top route; currently available) and real-time MRI-guided GdNCT (bottom route; currently not available).

Table 3. Number of Particles Generated per Isotope

isotope	NA (%) ^a	σ (barn)	NP ^b	position to damage cancer-cell nuclei	NP _{norm} ^c	NP _{RBE} ^d
¹⁵⁷ Gd	15.7	254000	5.0 ACK electrons +0.69 IC electrons +1.8 γ -rays = 7.49 particles	Inside (ACK and IC electrons and γ -rays) and outside (γ -rays) cancer cell	390.0	478.0 (sum of ¹⁵⁷ Gd + ¹⁵⁵ Gd)
¹⁵⁵ Gd	14.8	60700	5.0 ACK electrons +0.69 IC electrons +1.8 γ -rays = 7.49 particles	Inside (ACK and IC electrons and γ -rays) and outside (γ -rays) cancer cell	88.0	478.0 (sum of ¹⁵⁷ Gd + ¹⁵⁵ Gd)
¹⁰ B	19.9	3840	1.0 α + 1.0 ⁷ Li = 2.0 particles	Only inside cancer cell	2.0	40.0

^aNA = natural abundance. ^bNP = Number of particles generated per isotope. ^cNP_{norm} = Number of particles linearly normalized with respect to σ and NA of ¹⁰B. ^dNP_{RBE} = RBE weighting factor-weighted NP_{norm} (RBE weighting factor: γ -ray = electron = 1.0 and α -particle = ⁷Li = 20.0).²⁵

previous experiments, cancer was monitored *via* MRI before and after GdNCT. For example, Jung et al. used Gd(DO3A)-BTA in MDA-MB-231 cancer-bearing mice (Figure 5b),^{11j} Mi et al. used Gd-DTPA/CaP nanocomposites in C-26 cancer-bearing mice (Figure 8a and b),^{14a} and Ho et al. used Gd-nanoparticles in U87MG cancer-bearing mice (Figure 13a);^{17d} all of them observed cancer-growth suppressions after GdNCT *via* MRI. Real-time MRI-guided GdNCT will be fascinating because cancer status can be monitored during NCT. This will considerably improve cancer treatments *via* optimization of treatment conditions such as neutron beam and GdNCT agent injection doses (Figure 14).

6. DESIGN STRATEGY FOR GDNCT AGENTS IN CLINICAL USE

Substantial efforts have been made in the synthesis of various GdNCT agents to overcome the limitations of commercial Gd-chelates, such as extracellular^{20a} and non-cancer-targeting properties,⁹ causing poor accumulation in cancer cells.^{5,10a,11b,14b} All the GdNCT agents applied to *in vitro* (Table 1) and *in vivo* (Table 2) GdNCT experiments showed cancer-cell killing effects with a degree of efficacy, which depended on the GdNCT agent used (primarily on Gd-accumulation amount in cancer cells). These previous attempts indicate that GdNCT agents require careful designing and tailoring for further clinical applications. Therefore, they should cover (1) nontoxicity, (2) exclusive delivery to cancer cells *via* active cancer targeting, (3) sufficient Gd-delivery to cancer, (4) intravenous administration, and (5) renal excretion, as shown in Figure 15.

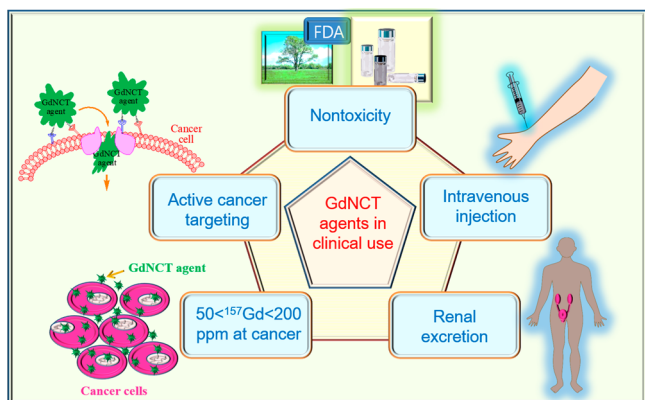


Figure 15. Design strategy of GdNCT agents for clinical applications. GdNCT agents require careful designing and tailoring for further clinical applications. They should cover (1) nontoxicity, (2) exclusive delivery to cancer cells *via* active cancer targeting, (3) sufficient Gd-delivery to cancer, (4) intravenous administration, and (5) renal excretion.

6.1. Nontoxicity. It is well-known that commercial MRI contrast agents can induce rare fibrosis in the skin, eyes, and internal organs of patients with impaired kidney function.²⁶ This disease is known as nephrogenic systemic fibrosis (NSF). It occurs when free Gd³⁺ ions are released from injected MRI contrast agents and deposited in the body.²⁶ Therefore, GdNCT agents should be unable to liberate free Gd³⁺ ions during GdNCT and should be excreted from the body through the renal system after GdNCT. Consequently, GdNCT agents should be synthesized to exhibit high kinetic stability. For Gd-chelates, Gd³⁺ ions should be strongly coordinated to chelates,

and Gd-nanoparticles should be tightly grafted with hydrophilic and biocompatible ligands.

6.2. Exclusive Delivery of GdNCT Agents to Cancer *via* Active Cancer Targeting. A main drawback in binary therapy, such as NCT, is that normal cells could be damaged during NCT because the radiation and NCT agents cannot be only exposed to the cancer cells. Hence, the incorporation of cancer-targeting ligands into GdNCT agents is highly desirable to achieve the selective delivery of GdNCT agents to cancer cells *via* active cancer targeting.²⁴

Cancer-targeting ligands generally bind to cancer cells through their interaction with specific receptors or transporters which are overexpressed on cancer-cell membranes.^{27a} There are many kinds of cancer-targeting ligands, which can be conjugated to GdNCT agents. These include small molecules, such as folic acid,^{27b} glucose,^{27c} L-type amino acid,^{27d} and anisamide-based compounds;^{27e} small peptides, such as RGDs;^{27f} large peptides or oligonucleotides, such as aptamers;^{27g} and biological molecules, such as antibodies.^{27h}

It is noteworthy that GdNCT agents conjugated with only one type of cancer-targeting ligand can only bind to the corresponding receptors overexpressed on cancer cells. This leads to a limited delivery of GdNCT agents to cancer cells because of receptor saturation.²⁷ⁱ If GdNCT agents are conjugated with various types of cancer-targeting ligands, they can bind to various types of receptors overexpressed on cancer cells,²⁷ⁱ thereby enhancing the delivery of GdNCT agents to cancer cells. Furthermore, the GdNCT efficacy can be improved if GdNCT agents penetrate cancer cells, preferably cancer-cell nuclei to enable short-range ACK and IC electrons to efficiently damage cancer-cell DNAs.⁴ However, if GdNCT agents are accumulated outside cancer-cell membranes, long-range γ -rays will mainly contribute to cancer-cell killing, and normal cells can also be damaged because of the long penetration depth (>1 cm) of γ -rays. Therefore, the combined conjugation of various types of cancer-targeting and cancer-cell penetrating ligands^{27j} to GdNCT agents is highly desirable in enhancing the efficacy of GdNCT.

6.3. Sufficient Delivery of GdNCT Agents to Cancer.

The optimal ¹⁵⁷Gd-amount in cancer was reported to be 50–200 μg ¹⁵⁷Gd/g cancer tissues (or 50–200 ppm),^{15a} but less than 1000 ppm ¹⁵⁷Gd because extra Gd only consumes thermal neutrons without contributing to cancer-cell killing.^{14b,15a} Furthermore, extra Gd can reduce GdNCT efficacy because of the shielding effects of thermal neutrons, as observed in dog treatments.¹¹ⁱ

The accumulation of ¹⁵⁷Gd in cancer cells can be increased in various ways. One is to conjugate cancer-targeting ligands to GdNCT agents, as previously mentioned. Another is to use ¹⁵⁷Gd-enriched GdNCT agents. The Gd-nanoparticles will be also useful for this because each nanoparticle can deliver tens to hundreds of ¹⁵⁷Gd to cancer cells.

6.4. Intravenous Injection. The injection route is important because the Gd-amount accumulated in cancer depends on it, as previously confirmed.²⁸ Although direct intratumoral injection can deliver a large amount of GdNCT agents to cancer, compared to intravenous injection, GdNCT agents should ideally be intravenously injected because it is generally difficult to deliver GdNCT agents to an exact cancer position *via* either intratumoral or intraperitoneal injections for deeply seated cancers in the body, such as brain cancer. After intravenous injection, GdNCT agents circulate through blood

vessels and accumulate at the cancer position *via* active targeting²⁴ or active and passive targeting;^{21h} the former applies to cancer-targeting ligand-conjugated Gd-chelates, and the latter applies to cancer-targeting ligand-conjugated Gd-nanoparticles and nanocomposites.

6.5. Renal Excretion. Injected GdNCT agents should be removed from the body after GdNCT treatment. The GdNCT agents can be excreted *via* the renal or hepatobiliary system, depending on their size.^{29a} Ideally, renal excretion is preferred because intact GdNCT agents can be excreted without modification or decomposition, whereas they may decompose if they are excreted *via* the hepatobiliary system. As previously mentioned, Gd³⁺ ions released in the body can cause side effects, such as NSF.²⁶ It is known that excretion through kidneys is limited by the filtration diameter of the kidneys, which is typically in the range of 4.5–5 nm.^{29b} Therefore, molecular agents can be excreted *via* the renal system. For nanoparticle agents, only those with tiny particle diameters (<3 nm) can be excreted *via* the renal system,^{29c} and hepatobiliary excretion increases as particle diameter increases. For example, 77.5% of intravenously injected gold nanoparticles with an average particle diameter of 1.9 nm were excreted *via* the renal system within 5 h after injection.^{29d} Therefore, nanoparticle GdNCT agents should be as small as possible in diameter for renal excretion.

7. CONCLUSION AND PERSPECTIVES

As reviewed, GdNCT is a new promising and noninvasive cancer therapeutic technique. As a binary therapy, a neutron beam source emitting thermal and epithermal neutrons and GdNCT agents are required. Neutron beam sources are relatively well-developed, compared to GdNCT agents. The available neutron beam sources include nuclear reactors, linear accelerators, and ring-cyclotron accelerators. The accelerators have been commercialized and are preferred for application in GdNCT, because they are more compact, safer, and cheaper than nuclear reactors and can be easily installed in hospitals and institutes.

There have been appreciable attempts to design and synthesize GdNCT agents to date, because commercial MRI contrast agents (Gd-chelates) are not suitable in clinical GdNCT applications because of their poor accumulation in cancer cells due to their noncancer targeting and extracellular properties and rapid excretion. Such GdNCT agents include modified Gd-chelates, nanocomposites containing Gd-chelates, fullerenes containing Gd, and solid-state Gd-nanoparticles. They were observed to exhibit higher accumulation in cancer cells, compared to commercial Gd-chelates; therefore, they demonstrated higher cancer-cell killing effects.


All previous GdNCT experiments showed GdNCT effects, and the degree of the effects depended on GdNCT agents used (primarily on Gd-accumulation amount in cancer cells). In addition, several experiments demonstrated better performance of GdNCT in cancer-cell killing, compared to BNCT. This is probably because GdNCT agents generate more particles to kill cancer cells, compared to BNCT agents; approximately ten times more RBE weighting factor-weighted particles are generated from both ¹⁵⁵Gd and ¹⁵⁷Gd, compared to ¹⁰B. Furthermore, GdNCT agents allow precise MRI-guided GdNCT.

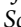
Considering all aforementioned outcomes, GdNCT is a promising cancer treatment technique. Therefore, more GdNCT agents should be synthesized and investigated.

Continuous efforts should be made to synthesize GdNCT agents, which are suitable in clinical use.


AUTHOR INFORMATION

Corresponding Authors

Gang Ho Lee – Department of Chemistry, College of Natural Sciences, Kyungpook National University, Taegu 41566, South Korea;  orcid.org/0000-0001-7451-6366; Email: ghlee@mail.knu.ac.kr

Yongmin Chang – Department of Molecular Medicine, School of Medicine, Kyungpook National University, Taegu 41405, South Korea;  orcid.org/0000-0002-0585-8714; Email: ychang@knu.ac.kr

Authors

Son Long Ho – Department of Chemistry, College of Natural Sciences, Kyungpook National University, Taegu 41566, South Korea;  orcid.org/0000-0001-7175-246X

Huan Yue – Department of Chemistry, College of Natural Sciences, Kyungpook National University, Taegu 41566, South Korea

Tirusew Tegafaw – Department of Chemistry, College of Natural Sciences, Kyungpook National University, Taegu 41566, South Korea

Mohammad Yaseen Ahmad – Department of Chemistry, College of Natural Sciences, Kyungpook National University, Taegu 41566, South Korea

Shuwen Liu – Department of Chemistry, College of Natural Sciences, Kyungpook National University, Taegu 41566, South Korea

Sung-Wook Nam – Department of Molecular Medicine, School of Medicine, Kyungpook National University, Taegu 41405, South Korea;  orcid.org/0000-0002-2306-6032

Complete contact information is available at:

<https://pubs.acs.org/10.1021/acsomega.1c06603>

Notes

The authors declare no competing financial interest.

Biographies



Son Long Ho currently serves as research professor in Prof. Gang Ho Lee's group in the Department of Chemistry at Kyungpook National University, where he obtained his Ph.D. degree (2015) under the supervision of Prof. Chan Sik Cho. Now his research interests focus on the development and application of lanthanide nanomaterials for MR imaging and gadolinium neutron capture therapy.



Huan Yue obtained her Ph.D. (2021) degree under the supervision of Prof. Gang Ho Lee in the Department of Chemistry at Kyungpook National University, where she continues her research as a postdoctoral research fellow. Her research interests focus on the complexation of europium and terbium by water-soluble lanthanide nanoparticles for MR and fluorescent imaging of viruses.



Shuwen Liu is currently a Ph.D student in Prof. Gang Ho Lee group in the Department of Chemistry at Kyungpook National University where she obtained her B.Sc. in 2015. Her researches focus on the development of ultrasmall lanthanide nanoparticles for MRI contrast agents with tumor targeting ability and fluorescent imaging of bacteria and viruses.



Tirusew Tegafaw obtained his Ph.D. (2016) degree under the supervision of Prof. Gang Ho Lee in the Department of Chemistry at Kyungpook National University, where he continues his career as a postdoctoral research fellow. His research interests focus on the development and application of core/shell nanomaterials for fluorescence and MRI imaging.



Sung-Wook Nam obtained his Ph.D. in materials science and engineering at Seoul National University, Republic of Korea. He worked as a postdoctoral researcher at University of Pennsylvania, IBM Watson Research Center, and a research fellow at Institute for Basic Science until 2016. He is currently an associate professor at School of Medicine, Kyungpook National University. His research is focused on design and fabrication of nanobio devices for diagnostic applications.



Mohammad Yaseen Ahmad obtained his Ph.D. (2020) degree under the supervision of Prof. Gang Ho Lee in the Department of Chemistry at Kyungpook National University, where he continues his career as a postdoctoral research fellow. His current research interests are the synthesis, characterization, and application of lanthanide nanomaterials for cancer diagnosis and treatment.



Yongmin Chang obtained his Ph.D. in condensed matter physics at the University of Notre Dame, USA, 1994 and worked as a research scientist at University of Illinois at Urbana—Champaign, USA. He is currently a professor in the Department of Molecular Medicine at the Kyungpook National University School of Medicine and in the

Department of Biomedical Engineering at the Kyungpook National University Graduate school, Korea, where his research is focused on synthesis, characterization, and molecular imaging applications of small molecular lanthanide complex.



Gang Ho Lee obtained his Ph.D. in physical chemistry at the Johns Hopkins University, USA, 1990, under the direction of Dr. Kit Bowen, Jr. and worked as a research scientist at Riken, Japan under the direction of Dr. Michio Takami. He is currently a professor in the Department of Chemistry at the Kyungpook National University, Korea, where his research is focused on synthesis, surface-functionalization, characterization, and biomedical applications of lanthanide oxide nanoparticles and composites.

ACKNOWLEDGMENTS

This work was supported by the Basic Science Research Program of the National Research Foundation (NRF) funded by the Ministry of Education, Science, and Technology (No. 2016R1D1A3B01007622) and by the NRF funded by the Korea government (Ministry of Science, and Information and Communications Technology: MSIT) (No. 2021R1A4A1029433).

NOTATIONS AND ABBREVIATIONS

$n+$, neutron beam irradiation; $n-$, no neutron beam irradiation; $Gd+$, with GdNCT agents; $Gd-$, no GdNCT agents; n , number of measurements; N , number of mice used in experiments; p , Student's t test in statistical analysis

REFERENCES

- (1) Siegel, R. L.; Miller, K. D.; Jemal, A. Cancer statistics. *CA Cancer J. Clin.* **2020**, *70*, 7–30.
- (2) Soloway, A. H.; Tjarks, W.; Barnum, B. A.; Rong, F.-G.; Barth, R. F.; Codogni, I. M.; Wilson, J. G. The chemistry of neutron capture therapy. *Chem. Rev.* **1998**, *98*, 1515–1562.
- (3) Dunning, J. R.; Pegram, G. B.; Fink, G. A.; Mitchell, D. P. Interaction of neutrons with matter. *Phys. Rev.* **1935**, *48*, 265–280.
- (4) (a) Martin, R. F.; D'Cunha, G.; Pardee, M.; Allen, B. J. Induction of DNA double-strand breaks by ^{157}Gd neutron capture. *Pigment Cell Res.* **1989**, *2*, 330–332. (b) Yokoya, A.; Ito, T. Photon-induced Auger effect in biological systems: a review. *Int. J. Radiat. Biol.* **2017**, *93*, 743–756.
- (5) De Stasio, G.; Rajesh, D.; Casalbone, P.; Daniels, M. J.; Erhardt, R. J.; Frazer, B. H.; Wiese, L. M.; Richter, K. L.; Sonderegger, B. R.; Gilbert, B.; et al. Are gadolinium contrast agents suitable for gadolinium neutron capture therapy? *Neurol. Res.* **2005**, *27*, 387–398.
- (6) (a) Locher, G. L. Biological effects and therapeutic possibilities of neutrons. *Am. J. Roentgenol. Radium. Ther.* **1936**, *36*, 1–13. (b) Barth, R. F.; Coderre, J. A.; Vicente, M. G. H.; Blue, T. E. Boron

neutron capture therapy of cancer: current status and future prospects. *Clin. Cancer Res.* **2005**, *11*, 3987–4003.

(7) Hosmane, N. S.; Maguire, J. A.; Zhu, Y.; Takagaki, M. *Boron and Gadolinium Neutron Capture Therapy for Cancer Treatment*; World Scientific Publishing: Singapore, 2012.

(8) Leinweber, G.; Barry, D. P.; Trbovich, M. J.; Burke, J. A.; Drindak, N. J.; Knox, H. D.; Ballard, R. V.; Block, R. C.; Danon, Y.; Severnyak, L. I. Neutron capture and total cross-section measurements and resonance parameters of gadolinium. *Nucl. Sci. Eng.* **2006**, *154*, 261–279.

(9) Wahsner, J.; Gale, E. M.; Rodríguez-Rodríguez, A.; Caravan, P. Chemistry of MRI contrast agents: current challenges and new frontiers. *Chem. Rev.* **2019**, *119*, 957–1057.

(10) (a) Geninatti-Crich, S.; Alberti, D.; Szabo, I.; Deagostino, A.; Toppino, A.; Barge, A.; Ballarini, F.; Bortolussi, S.; Bruschi, P.; Protti, N.; et al. MRI-guided neutron capture therapy by use of a dual gadolinium/boron agent targeted at tumour cells through upregulated low-density lipoprotein transporter. *Chem.—Eur. J.* **2011**, *17*, 8479–8486. (b) Alberti, D.; Protti, N.; Toppino, A.; Deagostino, A.; Lanzardo, S.; Bortolussi, S.; Altieri, S.; Voena, C.; Chiarle, R.; Crich, S. G.; et al. Theranostic approach based on the use of a dual boron/Gd agent to improve the efficacy of Boron Neutron Capture Therapy in the lung cancer treatment. *Nanomedicine* **2015**, *11*, 741–750. (c) Protti, N.; Geninatti-Crich, S.; Alberti, D.; Lanzardo, S.; Deagostino, A.; Toppino, A.; Aime, S.; Ballarini, F.; Bortolussi, S.; Bruschi, P.; Postuma, I.; Altieri, S.; Nikjoo, H. Evaluation of the dose enhancement of combined ^{10}B + ^{157}Gd neutron capture therapy (NCT). *Radiat. Prot. Dosimetry* **2015**, *166*, 369–373.

(11) (a) Hofmann, B.; Fischer, C.-O.; Lawaczek, R.; Platzek, J.; Semmler, W. Gadolinium neutron capture therapy (GdNCT) of melanoma cells and solid tumors with the magnetic resonance imaging contrast agent Gadobutrol. *Invest. Radiol.* **1999**, *34*, 126–133. (b) De Stasio, G.; Casalbone, P.; Pallini, R.; Gilbert, B.; Sanita, F.; Ciotti, M. T.; Rosi, G.; Festinesi, A.; Larocca, L. M.; Rinelli, A.; Perret, D.; Mogk, D. W.; Perfetti, P.; Mehta, M. P.; Mercanti, D. Gadolinium in human glioblastoma cells for gadolinium neutron capture therapy. *Cancer Res.* **2001**, *61*, 4272–4277. (c) Franken, N. A. P.; Bergs, J. W. J.; Kok, T. T.; Kuperus, R. R. N.; Stecher-Rasmussen, F.; Haveman, J.; Van Bree, C.; Stalpers, L. J. A. Gadolinium enhances the sensitivity of SW-1573 cells for thermal neutron irradiation. *Oncol. Rep.* **2006**, *15*, 715–720. (d) Tokuyue, K.; Tokita, N.; Akine, Y.; Nakayama, H.; Sakurai, Y.; Kobayashi, T.; Kanda, K. Comparison of radiation effects of gadolinium and boron neutron capture reactions. *Strahlenther. Onkol.* **2000**, *176*, 81–83. (e) Khokhlov, V. F.; Yashkin, P. N.; Silin, D. I.; Djorova, E. S.; Lawaczek, R. Neutron capture therapy with gadopentate dimeglumine: experiments on tumor-bearing rats. *Acad. Radiol.* **1995**, *2*, 392–398. (f) Matsumura, A.; Zhang, T.; Yamamoto, T.; Yishida, F.; Sakura, Y.; Shimojo, N.; Nose, T. In vivo gadolinium neutron capture therapy using a potentially effective compound (Gd-BOPTA). *Anticancer Res.* **2003**, *23*, 2451–2456. (g) Takagaki, M.; Hosmane, N. S. Gadolinium neutron capture therapy for malignant brain tumors. *Aino J.* **2007**, *6*, 39–44. (h) Yoshida, F.; Yamamoto, T.; Nakai, K.; Zaboronok, A.; Matsumura, A. Additive effect of BPA and Gd-DTPA for application in accelerator-based neutron source. *Appl. Radiat. Isot.* **2015**, *106*, 247–250. (i) Mitin, V. N.; Kulakov, V. N.; Khokhlov, V. F.; Sheino, I. N.; Arnopolskaya, A. M.; Kozlovskaya, N. G.; Zaitsev, K. N.; Portnov, A. A. Comparison of BNCT and GdNCT efficacy in treatment of canine cancer. *Appl. Radiat. Isot.* **2009**, *67*, S299–S301. (j) Jung, K.-H.; Park, J. - A.; Kim, J. Y.; Kim, M. H.; Oh, S.; Kim, H.-K.; Choi, E.-J.; Kim, H.-J.; Do, S. H.; Lee, K. C.; Kim, K. M.; Lee, Y. J. Image-guided neutron capture therapy using the Gd-DO3A-BTA complex as a new combinatorial treatment approach. *Contrast Media Mol. Imaging* **2018**, *2018*, 1–9.

(12) (a) Shikata, F.; Tokumitsu, H.; Ichikawa, H.; Fukumori, Y. In vitro cellular accumulation of gadolinium incorporated into chitosan nanoparticles designed for neutron-capture therapy of cancer. *Eur. J. Pharm. Biopharm.* **2002**, *53*, 57–63. (b) Fujimoto, T.; Ichikawa, H.; Akisue, T.; Fujita, I.; Kishimoto, K.; Hara, H.; Imabori, M.; Kawamitsu, H.; Sharma, P.; Brown, S. C.; Moudgil, B. M.; Fujii,

- M.; Yamamoto, T.; Kurosaka, M.; Fukumori, Y. Accumulation of MRI contrast agents in malignant fibrous histiocytoma for gadolinium neutron capture therapy. *Appl. Radiat. Isot.* **2009**, *67*, S355–S358.
- (c) Tokumitsu, H.; Ichikawa, H.; Fukumori, Y. Chitosan-gadopentetic acid complex nanoparticles for gadolinium neutron-capture therapy of cancer: Preparation by novel emulsion-droplet coalescence technique and characterization. *Pharm. Res.* **1999**, *16*, 1830–1835. (d) Tokumitsu, H.; Hiratsuka, J.; Sakuragi, Y.; Kobayashi, T.; Ichikawa, H.; Fukumori, Y. Gadolinium neutron-capture therapy using novel gadopentetic acid-chitosan complex nanoparticles: in vivo growth suppression of experimental melanoma solid tumor. *Cancer Lett.* **2000**, *150*, 177–182. (e) Ichikawa, H.; Uneme, T.; Andoh, T.; Arita, Y.; Fujimoto, T.; Suzuki, M.; Sakurai, Y.; Shinto, H.; Fukasawa, T.; Fujii, F.; Fukumori, Y. Gadolinium-loaded chitosan nanoparticles for neutron-capture therapy: Influence of micrometric properties of the nanoparticles on tumor-killing effect. *Appl. Radiat. Isot.* **2014**, *88*, 109–113.
- (13) (a) Kobayashi, H.; Kawamoto, S.; Saga, T.; Sato, N.; Ishimori, T.; Konishi, J.; Ono, K.; Togashi, K.; Brechbiel, M. W. Avidin-dendrimer-(1B4M-Gd)254: A tumor-targeting therapeutic agent for gadolinium neutron capture therapy of intraperitoneal disseminated tumor which can be monitored by MRI. *Bioconjugate Chem.* **2001**, *12*, 587–593. (b) Qin, C.; Hou, X.; Khan, T.; Nitta, N.; Yanagawa, M.; Sakurai, Y.; Suzuki, M.; Masunaga, S.-I.; Tanaka, H.; Sakurai, Y.; et al. Enhanced MRI-guided gadolinium(III) neutron capture therapy by polymeric nanocarriers promoting tumor accumulation and intracellular delivery. *ChemNanoMater.* **2020**, *6*, 412. (c) Akine, Y.; Tokita, N.; Tokuyue, K.; Satoh, M.; Fukumori, Y. Neutron-capture therapy of murine ascites tumor with gadolinium-containing microcapsules. *J. Cancer Res. Clin. Oncol.* **1992**, *119*, 71–73.
- (14) (a) Mi, P.; Dewi, N.; Yanagie, H.; Kokuryo, D.; Suzuki, M.; Sakurai, Y.; Li, Y.; Aoki, I.; Ono, K.; Takahashi, H.; Cabral, H.; et al. Hybrid calcium phosphate-polymeric micelles incorporating gadolinium chelates for imaging-guided gadolinium neutron capture tumor therapy. *ACS Nano* **2015**, *9*, 5913–5921. (b) Dewi, N.; Mi, P.; Yanagie, H.; Sakurai, Y.; Morishita, Y.; Yanagawa, M.; Nakagawa, T.; Shinohara, A.; Matsukawa, T.; Yokoyama, K.; et al. In vivo evaluation of neutron capture therapy effectivity using calcium phosphate-based nanoparticles as Gd-DTPA delivery agent. *J. Cancer Res. Clin. Oncol.* **2016**, *142*, 767–775.
- (15) (a) Le, M.; Cui, U. Z. Biodistribution and tumor-accumulation of gadolinium (Gd) encapsulated in long-circulating liposomes in tumor-bearing mice for potential neutron capture therapy. *Int. J. Pharm.* **2006**, *320*, 96–103. (b) Dewi, N.; Yanagie, H.; Zhu, H.; Demachi, K.; Shinohara, A.; Yokoyama, K.; Sekino, M.; S, Y.; Morishita, Y.; Iyomoto, N.; Nagasaki, T.; et al. Tumor growth suppression by gadolinium-neutron capture therapy using gadolinium-entrapped liposome as gadolinium delivery agent. *Biomed. Pharmacother.* **2013**, *67*, 451–457. (c) Peters, T.; Grunewald, C.; Blaickner, M.; Ziegner, M.; Schütz, C.; Iffland, D.; Hampel, G.; Nawroth, T.; Langguth, P. Cellular uptake and in vitro antitumor efficacy of composite liposomes for neutron capture therapy. *Radiat. Oncol.* **2015**, *10*, 52–65. (d) Lee, W.; Jung, K. - H.; Park, J. - A.; Kim, J. Y.; Lee, Y. J.; Chang, Y.; Yoo, J. In vivo evaluation of PEGylated-liposome encapsulating gadolinium complexes for gadolinium neutron capture therapy. *Biochem. Biophys. Res. Commun.* **2021**, *568*, 23–29.
- (16) Horiguchi, Y.; Kudo, S.; Nagasaki, Y. Gd@C82 metallofullerenes for neutron capture therapy-fullerene solubilization by poly(ethylene glycol)-block-poly(2-(N,N-diethylamino)ethyl methacrylate) and resultant efficacy in vitro. *Sci. Technol. Adv. Mater.* **2011**, *12*, 044607–044614.
- (17) (a) Hwang, K. C.; Lai, P. D.; Chiang, C.-S.; Wang, P.-J.; Yuan, C.-J. Neutron capture nuclei-containing carbon nanoparticles for destruction of cancer cells. *Biomaterials* **2010**, *31*, 8419–8425. (b) Bridot, J. L.; Dayde, D.; Riviere, C.; Mandon, C.; Billotey, C.; Lerondel, S.; Sabattier, R.; Cartron, G.; Pape, A. L.; et al. Hybrid gadolinium oxide nanoparticles combining imaging and therapy. *J. Mater. Chem.* **2009**, *19*, 2328–2335. (c) Ho, S. L.; Cha, H.; Oh, I. T.; Jung, K.-H.; Kim, M. H.; Lee, Y. J.; Miao, X.; Tegafaw, T.; Ahmad, M. Y.; et al. Magnetic resonance imaging, gadolinium neutron capture therapy, and tumor cell detection using ultrasmall Gd₂O₃ nanoparticles coated with polyacrylic acid-rhodamine B as a multifunctional tumor theragnostic agent. *RSC Adv.* **2018**, *8*, 12653–12665. (d) Ho, S. L.; Choi, G.; Yue, H.; Kim, H.-K.; Jung, K.-H.; Park, J. A.; Kim, M. H.; Lee, Y. J.; Kim, J. Y.; Miao, X.; et al. In vivo neutron capture therapy of cancer using ultrasmall gadolinium oxide nanoparticles with cancer-targeting ability. *RSC Adv.* **2020**, *10*, 865–874.
- (18) (a) He, J.; Yang, L.; Hou, X.; Mester, Z.; Meija, J. Determination of the isotopic composition of gadolinium using multicollector inductively coupled plasma mass spectrometry. *Anal. Chem.* **2020**, *92*, 6103–6110. (b) Stepanek, J. Emission spectra of gadolinium-158. *Med. Phys.* **2003**, *30*, 41–43. (c) Tanaka, T.; Hagiwara, K.; Gazzola, E.; Ali, A.; Ou, L.; Sudo, T.; Das, P. K.; Reen, M. S.; Dhir, R.; Koshio, Y.; et al. Gamma-ray spectra from thermal neutron capture on gadolinium-155 and natural gadolinium. *Prog. Theor. Exp. Phys.* **2020**, *2020*, 043D02.
- (19) (a) Altieri, S.; Protti, N. A brief review on reactor-based neutron sources for boron neutron capture therapy. *Ther. Radiol. Oncol.* **2018**, *2*, 47. (b) Kiyonagi, Y. Accelerator-based neutron source for boron neutron capture therapy. *Ther. Radiol. Oncol.* **2018**, *2*, 55. (c) Yamamoto, T.; Tsuboi, K.; Nakai, K.; Kumada, H.; Sakurai, H.; Matsumura, A. Boron neutron capture therapy for brain tumors. *Transl. Cancer Res.* **2013**, *2*, 80–86. (d) Zhang, Z.; Liu, T. A review of the development of In-Hospital Neutron Irradiator-1 and boron neutron capture therapy clinical research on malignant melanoma. *Ther. Radiol. Oncol.* **2018**, *2*, 49. (e) Diaz, A. Z. Assessment of the results from the phase I/II boron neutron capture therapy trials at the Brookhaven National Laboratory from a clinician's point of view. *J. Neurooncol.* **2003**, *62*, 101–109. (f) Kueffer, P. J.; Maitz, C. A.; Khan, A. A.; Schuster, S. A.; Shlyakhtina, N. I.; Palisatgi, S. S.; Brockman, J. D.; Nigg, D. W.; Hawthorne, M. F. Boron neutron capture therapy demonstrated in mice bearing EMT6 tumors following selective delivery of boron by rationally designed liposomes. *Proc. Natl. Acad. Sci. U.S.A.* **2013**, *110*, 6512–6517.
- (20) (a) Morcos, S. K. Extracellular gadolinium contrast agents: differences in stability. *Eur. J. Radiol.* **2008**, *66*, 175–179. (b) Tartaro, A.; Maccarone, M. T. The utility of gadoteric acid in contrast-enhanced MRI: a review. *Rep. Med. Imaging* **2015**, *8*, 25–35. (c) Kirchin, M. A.; Pirovano, G. P.; Spinazzi, A. Gadobenate dimeglumine (Gd-BOPTA): an overview. *Invest. Radiol.* **1998**, *33*, 798–809.
- (21) (a) Kim, H.-K.; Kang, M.-K.; Jung, K.-H.; Kang, S.-H.; Kim, Y.-H.; Jung, J. - C.; Lee, G. H.; Chang, Y.; Kim, T. - J. Gadolinium complex of DO3A-benzothiazole aniline (BTA) conjugate as a theragnostic agent. *J. Med. Chem.* **2013**, *56*, 8104–8111. (b) Agrawal, P.; Strijkers, G. J.; Nicolay, K. Chitosan-based systems for molecular imaging. *Adv. Drug. Delivery Rev.* **2010**, *62*, 42–58. (c) Moura, L.I. F.; Malfani, A.; Peres, C.; Matos, A. I.; Guegain, E.; Sainz, V.; Zloh, M.; Vicent, M. J.; Florindo, H. F. Functionalized branched polymers: promising immunomodulatory tools for the treatment of cancer and immune disorders. *Mater. Horiz.* **2019**, *6*, 1956. (d) Yao, Z.; Zhang, M.; Sakahara, H.; Saga, T.; Arano, Y.; Konishi, J. Avidin targeting of intraperitoneal tumor xenografts. *J. Natl. Cancer Inst.* **1998**, *90*, 25–29. (e) Skwarczynski, M.; Zhao, G.; Boer, J. C.; Ozberk, V.; Azuar, A.; Cruz, J. G.; Giddam, A. K.; Khalil, Z. G.; Pandey, M.; Shibu, M. A.; et al. Poly(amino acids) as a potent self-adjuvanting delivery system for peptide-based nanovaccines. *Sci. Adv.* **2020**, *6*, eaax2285. (f) Liu, N.; Li, B.; Gong, C.; Liu, Y.; Wang, Y.; et al. A pH- and thermo-responsive poly(amino acid)-based drug delivery system. *Colloids Surf. B Biointerfaces* **2015**, *136*, 562–569. (g) Webber, M. J.; Appel, E. A.; Vinciguerra, B.; Cortinas, A. B.; Thapa, L. S.; Jhunjhunwala, S.; Isaacs, L.; Langer, R.; Anderson, D. G. Supramolecular PEGylation of biopharmaceuticals. *Proc. Natl. Acad. Sci. U.S.A.* **2016**, *113*, 14189–14194. (h) Nichols, J. W.; Bae, Y. H. EPR: Evidence and fallacy. *J. Controlled Release* **2014**, *190*, 451–464. (i) Sanchez-Lafuente, C.; Teresa Fauci, M.; Fernandez-Arevalo, M.; Alvarez-Fuentes, J.; Rabasco, A. M.; Mura, P. Development of sustained release matrix

tablets of didanosine containing methacrylic and ethylcellulose polymers. *Int. J. Pharm.* **2002**, *234*, 213–221. (j) Huang, D.; Mi, P. Calcium phosphate nanocarriers for drug delivery to tumors: imaging, therapy and theranostics. *Biomater. Sci.* **2019**, *7*, 3942–3960. (k) Allen, T. M.; Cullis, P. R. Liposomal drug delivery systems: From concept to clinical applications. *Adv. Drug. Delivery Rev.* **2013**, *65*, 36–48.

(22) (a) Shinohara, H. Another big discovery—metallofullerenes. *Philos. Trans. R. Soc. A* **2016**, *374*, 20150325. (b) Anderson, R. G. W.; Kamen, B. A. Potocytosis-sequestration and transport of small molecules by caveolae. *Science* **1992**, *255*, 410–411. (c) Weiss, H. V.; Shipman, W. H. Biological concentration by killer clams of cobalt-60 from radioactive fallout. *Science* **1957**, *125*, 695.

(23) Dong, H.; Du, S.-R.; Zheng, X.-Y.; Lyu, G.-M.; Sun, L.-D.; Li, L. D.; Zhang, P.-Z.; Zhang, C.; Yan, C.-H. Lanthanide nanoparticles: from design toward bioimaging and therapy. *Chem. Rev.* **2015**, *115*, 10725–10815.

(24) Attia, M. F.; Anton, N.; Wallyn, J.; Omran, Z.; Vandamme, T. F. An overview of active and passive targeting strategies to improve the nanocarriers efficiency to tumour sites. *J. Pharm. Pharmacol.* **2019**, *71*, 1185–1198.

(25) Valentin, J. *The 2007 Recommendations of the International Commission on Radiological Protection*; Annals of the ICRP Publication 103; Elsevier: Amsterdam, The Netherlands, 2007; pp 64.

(26) Colletti, P. M. Nephrogenic systemic fibrosis and gadolinium: a perfect storm. *Am. J. Roentgenol.* **2008**, *191*, 1150–1153.

(27) (a) Srinivasarao, M.; Low, P. S. Ligand-targeted drug delivery. *Chem. Rev.* **2017**, *117*, 12133–12164. (b) Fernandez, M.; Javaid, F.; Chudasama, V. Advances in targeting the folate receptor in the treatment/imaging of cancers. *Chem. Sci.* **2018**, *9*, 790–810. (c) Gui, L.; Yuan, Z.; Kassaye, H.; Zheng, J.; Yao, Y.; Wang, F.; He, Q.; Shen, Y.; Liang, L.; Chen, H. A tumor-targeting probe based on a mitophagy process for live imaging. *Chem. Commun.* **2018**, *54*, 9675–9678.

(d) Puris, E.; Gynther, M.; Auriola, S.; Huttunen, K. M. L-type amino acid transporter I as a target for drug delivery. *Pharm. Res.* **2020**, *37*, 88.

(e) Dasargyri, A.; Kümin, C. D.; Leroux, J.-C. Targeting nanocarriers with anisamide: fact or artifact? *Adv. Mater.* **2017**, *29*, 1603451. (f) Alipour, M.; Baneshi, M.; Hosseinkhani, S.; Mahmoudi, R.; Arabzadeh, A. J.; Akrami, M.; Mehrzad, J.; Bardania, H. Recent progress in biomedical applications of RGD-based ligand: From precise cancer theranostics to biomaterial engineering: A systematic review. *J. Biomed. Mater. Res.* **2020**, *108*, 839–850. (g) Yoon, S.; Rossi, J. J. Aptamers: Uptake mechanisms and intracellular applications. *Adv. Drug Delivery Rev.* **2018**, *134*, 22–35. (h) Sapra, P.; Shor, B. Monoclonal antibody-based therapies in cancer: Advances and challenges. *Pharmacol. Ther.* **2013**, *138*, 452–469. (i) Jang, C.; Lee, J. H.; Sahu, A.; Tae, G. The synergistic effect of folate and RGD dual ligand of nanographene oxide on tumor targeting and photothermal therapy in vivo. *Nanoscale* **2015**, *7*, 18584–18594. (j) Fonseca, S. B.; Perreira, M. P.; Kelly, S. O. Recent advances in the use of cell-penetrating peptides for medical and biological applications. *Adv. Drug Delivery Rev.* **2009**, *61*, 953–964.

(28) Watanabe, T.; Ichikawa, H.; Fukumori, Y. Tumor accumulation of gadolinium in lipid-nanoparticles intravenously injected for neutron-capture therapy of cancer. *Eur. J. Pharm. Biopharm.* **2002**, *54*, 119–124.

(29) (a) Longmire, M.; Choyke, P. L.; Kobayashi, H. Clearance properties of nano-sized particles and molecules as imaging agents: considerations and caveats. *Nanomedicine* **2008**, *3*, 703–717. (b) Ohlson, M.; Sorensson, J.; Haraldsson, B. A gel-membrane model of glomerular charge and size selectivity in series. *Am. J. Physiol. Renal. Physiol.* **2001**, *280*, F396–F405. (c) Soo Choi, H.; Liu, W.; Misra, P.; Tanaka, E.; Zimmer, J. P.; Iyiti Ipe, B.; Bawendi, M. G.; Frangioni, J. V Renal clearance of quantum dots. *Nat. Biotechnol.* **2007**, *25*, 1165–1170. (d) Hainfeld, J. F.; Slatkin, D. N.; Focella, T. M.; Smilowitz, H. M. Gold nanoparticles: a new X-ray contrast agent. *Br. J. Radiol.* **2006**, *79*, 248–253.